KERNFORSCHUNGSZENTRUM

KARLSRUHE

Juni 1972

KFK 1612

Institut für Angewandte Reaktorphysik
Institut für Neutronenphysik und Reaktortechnik
Projekt Schneller Brüter

Physiks Investigations of Sodium Cooled Fast Reactors SNEAK-Assemblies 6A/6B

G. Jourdan, F. Plum, H. Reichel

GESELLSCHAFT FÜR KERNFORSCHUNG M. B. H.

KARLSRUHE

GESELLSCHAFT FÜR KERNFORSCHUNG M. B. H.
KARLSRUHE

KERNFORSCHUNGSZENTRUM KARLSRUHE

June 1972 KFK 1612

Institut für Angewandte Reaktorphysik

Institut für Neutronenphysik und Reaktortechnik

Projekt Schneller Brüter

Physics Investigations of Sodium Cooled Fast Reactors

SNEAK-Assemblies 6A/6B

G. Jourdan, F. Plum, H. Reichel[1)]

With contributions from

W. Bickel, H. Bluhm, R. Böhme, R. Buyl[2)], G. Fieg, E.A. Fischer, F. Helm, P.E. Mc Grath, S. Pilate[3)], W. Scholtyssek, J. Voß[1)], H. Walze, U. Wehmann[1)], H. Werle, G. Wittek

1) Interatom
2) Euratom
3) Belgonucleaire

Gesellschaft für Kernforschung mbH., Karlsruhe

Abstract

SNEAK Assembly 6 was aimed at measuring physics parameters of a fast sodium cooled breeder core having a number of features typical for the prototype SNR. Whereas in SNEAK-Assembly 2 /1/ particular attention was given to a close simulation of the radial geometry, in SNEAK-Assembly 6 the axial behavior of the prototype SNR was simulated and studied. SNEAK-Assembly 6 had three modifications SNEAK-6A, SNEAK-6B and SNEAK-6D. SNEAK-6A has three zones, an inner Pu-zone with SNEAK material, a buffer zone composed of MASURCA rodlet material and the outer uranium zone. SNEAK-6B had the same zones without the buffer zone; in both assemblies some identical experiments were performed for studying the influence of the buffer zone. SNEAK-6D was a core with an inner Pu-zone with MASURCA material, a buffer zone, and a uranium driver zone. In this case the buffer zone was composed of SNEAK-material. The influence of the material geometry on some experiments was studied by comparing the results of these experiments in SNEAK-6A and 6D. The experimental results were compared to detailed calculations.

The work covered by this report was performed in close cooperation between the Gesellschaft für Kernforschung, the industrial consortium for the SNR and the French MASURCA group at Cadarache.

7. Juni 1972

Zusammenfassung

Die Anordnung SNEAK-6 diente der physikalischen Untersuchung eines schnellen natriumgekühlten Brüter-Cores, das wesentliche Züge des Prototyps SNR trug. Während in SNEAK-2 die radiale Geometrie des SNR so gut wie möglich simuliert wurde, wurde in SNEAK-6 das axiale Verhalten des SNR angenähert und studiert. SNEAK-6 bestand aus 3 Corekonfigurationen: SNEAK-6A, 6B und 6D. SNEAK-6A war ein Core mit einer SNEAK-Pu-Plättchen-Innenzone, einer Pufferzone aus MASURCA-Material und einer Urantreiberzone; 6B ein Core mit derselben Pu-Innenzone und derselben Treiberzone, während die Pufferzone fehlte; in beiden Anordnungen wurden ähnliche Experimente durchgeführt, um den Einfluß der Pufferzone zu studieren. SNEAK-6D war ein Core mit einer Pu-Innenzone aus MASURCA-Material, einer Pufferzone aus SNEAK-Material und der Urantreiberzone. Durch Vergleich von ähnlichen Experimenten in SNEAK-6A und 6D sollte der Einfluß der Materialgeometrie studiert werden. Die experimentellen Ergebnisse wurden mit detaillierten Berechnungen verglichen.

Die in diesem Bericht beschriebenen Arbeiten wurden in enger Zusammenarbeit zwischen der Gesellschaft für Kernforschung, dem Industriekonsortium SNR und der französischen MASURCA-Gruppe in Cadarache durchgeführt.

Contents

1. Introduction

The series of assemblies SNEAK-6 was designed for investigating physics parameters in a core environment typical for the inner zone of a sodium cooled fast core of the SNR-type. Of particular interest were also the influence of platelet- and rodlet geometry of the fuel and of the dimensions of the core zone in which experiments were performed on the results of the essential measurements. Uranium and plutonium fuel was used.

Design and evaluation of the experiments were performed in close cooperation between the Institut für Angewandte Reaktorphysik of the Kernforschungszentrum Karlsruhe and the industrial consortium for the construction of the SNR and partially as common experiment with French scientists of the fast critical facility MASURCA. For several months about 90 kg of plutonium from MASURCA were used in SNEAK. Since MASURCA materials are in the form of rodlets while SNEAK is using platelets some effort had to be made to adapt the compositions. Finally the cells built of SNEAK-platelets could be arranged in such a way that the integral composition of the unit cells formed with MASURCA rodlets were well matched. The experimental program concentrated on the axial measurements of most interest in the present design status of the SNR - such as axial power distribution, sodium void measurements and the reactivity worth of central control rods.

The program was subdivided into three assemblies which are briefly described in the following.

SNEAK-6A was a cylindrical core with an inner plutonium zone surrounded by a buffer zone built with MASURCA rodlets and also fueled with plutonium. The outer zone was an uranium driver zone in which spectra and B_m^2 was adjusted to the values of the inner zone. After some basic measurements (critical data, reaction rates, material worth, axial void traverses, spectra) the buffer zone was substituted by the uranium driver composition. In this new assembly (SNEAK-6B) some important measurements were repeated. SNEAK-6D was the last configuration of the three assemblies. The inner zone of this configuration was built with MASURCA rodlet material, the buffer zone with SNEAK platelets and this zone again was surrounded by the uranium driver zone. The experiments in this assembly were mostly the same as in SNEAK-6A and by comparing the results one can obtain some informations of the influence of the material geometry.

The experimental work on SNEAK-6 started in February 1970 and was completed in September of the same year.

2. General description of the experimental techniques

Most of the experimental techniques applied in SNEAK-6 experiments were already utilized during the SNEAK-2 experiments. These are described in /1/. Some additional methods will be described here.

2.1 Reaction rate measurements

Axial and radial reaction rate distributions were measured with fission chambers and by foil activations. In the SNEAK-6A and 6B axial measurements, Pu-, Np-, U^{235}- and U^{238}-fission chambers with a diameter of 8 mm, developed in Cadarache, could be used. For the radial measurements in SNEAK-6A and 6B, Pu^{239}, U^{235}- and U^{238} fission chambers with a diameter of 6,35 mm (Type FC4, 20^{th} Century Electronics) were used. In addition to the main isotope the chamber deposits contained the impurities given in Table 6. The more accurate and detailed measurements were performed in the axial direction, in the upper half of the core and axial breeder blanket. For these measurements in position 17/20 a special element was used loaded with platelets with a central hole resulting in a vertical channel within the element. The results of the chamber measurements were corrected for the effect of the dead time (~3,2 µsec). The correction for the presence of impurities is negligible (< 0.1 %).
The U^{235}- and U^{238}-fission rate and the U^{238}-capture rate were also measured with pairs of pure uranium metal foils (20,04 $^{w}/o$ and 0,44 $^{w}/o$ U^{235}).
^{239}Pu fission rates were determined from irradiated foils of a Pu-Aluminium alloy.
During the irradiation the foils were placed between the platelets of a unit cell. After the irradiation, the capture rate of ^{238}U was obtained by counting the coincidences of γ-rays and x-rays of decaying ^{239}Pu levels at energies ~100 keV.

The ratio of ^{238}U capture to ^{235}U fission was calibrated by simultaneous irradion of a pair of foils in the thermal spectrum of the Cadarache Harmonie reactor. Counting the γ-activity of fission products > 660 keV γ-energy yielded information about the fission rate in the foils /2/.

2.2 Neutron spectra measurements

Neutron spectra measurements were performed in the center of SNEAK-6A (position 17/20).

To determine neutron spectra resonance absorber foils /3/, proton-recoil counters /5/, /6/, Li-6 semiconductor spectrometers /4/ and a He-3 sandwich spectrometer /5/ were used. Some improvements applied are described in /7/.

For the semiconductor spectrometer measurements, the reactor was taken critical. For measurements with the recoil counters, the reactor was fully shut down (shim, regulating and safety rods fully inserted) to assure that sufficiently low count rates were reached. Measuring in the subcritical region, a count rate below 3000 pulses/sec assures satisfactory functioning of the electronics.

2.3 Cavity measurements

Of interest are the nuclear safety aspects of cavity zones created by reactions between fuel and sodium and their influence on reactivity changes. Cavities were simulated both in the center of the core and in excentric positions. The SNEAK core elements were reloaded in four steps (Fig. 15).

a) A sodium void zone was created comprising four SNEAK core fuel elements over a height of 42.9 cm, by exchanging Na-platelets against empty platelets.

b) In the same way additional void position were created axially and radially adjacent to the original void zone providing sufficient space the accomodate all fuel and structural platelets of the original zone.

c) Fuel material (PuO_2 UO_2 platelets) was extracted from the cavity zone (original void zone) and redistributed in the void positions provided in step b) along the periphery of the cavity.

d) All steel, uranium and ferrous platelets were removed from the cavity zone and redistributed in the void positions along the cavity periphery. To support the materials above the cavity zone aluminium spacers of various thicknesses were inserted. This made it possible to evaluate the effect of creating a completely empty space in the tubes via extrapolation.

The reactivity change caused by each rearrangement step, was measured with the calibrated SNEAK shim rods.

3. General description of the calculational methods

3.1 Methods of current use

The SNEAK-6 evaluations were generally performed using the methods already used for SNEAK-2 and described in Chapter 3 of /1/. These methods will not be described in detail here again.

First one must say that some experiments were evaluated from different groups (GFK, Belgonucleaire, INTERATOM). Therefore the evaluation of some experiments is inconsistent (for instance the evaluation of the radial and axial reaction rate traverses was done with different cross section sets).

The cross-section sets used were again the Karlsruhe 26-group sets NAPPMB /8/ and MOXTOT /9/, but their respective roles have been inversed since SNEAK-2, MOXTOT being now considered as the basis set and NAPPMB being employed additionally in order to make easier the comparison of results between SNEAK-2 and -6.

Diffusion theory was again used in the whole series of calculations but there was an increased additional application of transport methods as a complement. To the list of computer programs given in /1/, one has to add the program SNOW /10/, developed by GfK, which solves the two-dimensional transport equations with the S_n approximation; this code presents some practical advantages when compared to similar existing codes /11/.

The cavity experiments which are described and evaluated in Chapter 4.10 were a particularly delicate case of application of the two-dimensional diffusion and transport programs. The presence of the cavity was simulated by a scattering medium of very low density.

The next two paragraphs 3.2 and 3.3 present the newly developed methods applied to SNEAK-6: the 208-group formalism and the KAPER program.

3.2 The 208-group formalism

Group constants were prepared at Karlsruhe in a 208-group scheme in the frame of the P_1 approximation /12/. Such a fine energy subdivision is needed to correctly account for the elastic scattering processes in light media, and for the threshold reactions. The data set GRUBA includes these constants for all the isotopes entering the usual 26-group sets.

This formalism was primarily developed in order to better evaluate the neutron spectrum measurements. Results of such an application are given in Chapter 4.

3.3 The "KAPER" Program

The KAPER program /13/ was written at Karlsruhe in order to calculate fluxes, reaction rates and material worths in the plate geometry of the SNEAK cores. It is based on the collision probability method, as the programs ZERA /14/ and REAC /15) of which it represents an extension and an improvement. KAPER allows to consider not only the normal unperturbed cell of the lattice but

also the cell which is perturbed by the experiment (presence of a channel, of activation foils or of samples), by a special source algorithm.

KAPER was applied to the calculation of material worths and of the cell fine structure in SNEAK-6A (see Chapter 4).

4. Assembly SNEAK-6A/6B

4.1 Description of the geometries and compositions of both core configurations

4.1.1 SNEAK-6A

Assembly SNEAK-6A had three core zones.

a) The central Pu-zone Z1A was filled with SNEAK platelets. The height of this core zone was 90 cm.

b) The next zone Z1MAS was a Pu-zone also, and was filled with MASURCA-material to a height of 60 cm (centered on the core mid-plane) which corresponds to the length of the MASURCA-Pu rodlets. The average composition was the same as that of the SNEAK-Pu zone Z1A. The top and bottom (15 cm) of this core zone were filled with the uranium composition R1.

c) The outer core zone was the uranium driver zone R1. The height of this core zone was 90 cm also.

The upper and lower axial blanket for all zones had a composition which simulated a breeder blanket of a power reactor. There were two cells for the breeder blanket. One was used for the zones Z1A and Z1MAS, the other which was modified (the sodium platelet of the cell was replaced by one Al-100 % platelet and two SS-40 % platelets) was used for the R1 zone. The radial blanket was depleted uranium. The SNEAK control rods were fueled with the composition R1, because only a few small-sized Pu platelets are available. The position of these rods was selected in such a way that the uranium filling would not perturb the experiments. Fig. 9 and 10 show a vertical and a horizontal section

through the critical configuration of the assembly SNEAK-6A, together with the critical dimensions which were used in the calculations. The core zone Z1A was subdivided in two concentric parts, Z1A' and Z1A, because the compositions for the k_{eff}-calculations for the two zones were different. The composition for the inner zone Z1A' takes into account only the unit cells and the rest cells used at the upper and lower core boundary. The composition of the zone Z1A includes the SNEAK control rods which were positioned in this zone.
Fig. 1a - 1g show the structure of the unit cells used in each zone and the rest cells; Fig. 2 shows the structure of the unit- and rest cells of the SNEAK control rods.
Tables 1a - 1b give the composition of each reactor zone. Two types of compositions are shown: The first one is the composition for the k_{eff}-calculation; it includes the contributions of the unit cells, the SNEAK control rods in their respective zones and the rest cells. The second type was used for the calculation of the reaction rates; it corresponds to the composition of the unit cells.

4.1.2 Configuration SNEAK-6B

SNEAK-6B had only two core zones. The Z1MAS zone of SNEAK-6A was removed and this part of the core was also fueled with the R1 composition. The zone Z1A was enlarged by one element (in the position 11/17).

Fig. 11 and 12 show a vertical and a horizontal cross section through the critical core configuration.
Tables 2a - b give the k_{eff}-compositions for each reactor zone. The compositions for the reaction rate calculations were the same as in SNEAK-6A.

4.2 Critical Experiment of SNEAK-6A and 6B

4.2.1 Experimental results

Fig. 9 shows a cross section of the critical configuration of SNEAK-6A; Fig. 11 the same for SNEAK-6B. All SNEAK control-rods are in their most reactive position.

The measured k_{eff} values were:

	SNEAK-6A	SNEAK-6B
k_{eff}:	1.0003	1.0000

4.2.2 Methods and results of the k_{eff} calculations

The calculations for the critical experiments were performed with the methods, which are described in more detail in chapter 3. The basic calculations was in each case a two dimensional homogeneous diffusion calculation with 26 groups in R-Z geometry. Figs. 10 and 12 show the geometry, and Tables 1 and 2 the compositions utilized. The average mesh size was 1 cm for the core zone and 2 - 3 cm for the blanket region. The numerical accuracy of the calculations was 1.10^{-4} in k_{eff}.
Some corrections were computed in one or zero dimensional geometry and 26 groups.

a) transport correction (S_8-correction)

b) heterogeneity correction (influence of the cell structure)

c) REMO correction (Improvement of the elastic removal cross sections in the first 14 energy groups)

A correction for cylindrisation was found by comparing a one dimensional cylindrical diffusion calculation with a two dimensional x-y diffusion calculation, both with the same axial bucklings. All calculations were performed with the MOXTOT /9/ cross section set. Some important calculations were repeated with the NAPPMB /8/ cross section set.
Table 9 lists the results of these calculations.
One observes that in the case of SNEAK-6A both cross section sets produce a slight underestimate in k_{eff} while in the case of SNEAK-6B the MOXTOT cross section set overestimates k_{eff}. This reflects the fact that MOXTOT tends to overestimate the reactivity of uranium fuelled compositions. The result of the NAPPMB cross-section set is negligibly influenced.

4.3 Spectra measurements

4.3.1 Experimental results

The spectrum of the central zone of SNEAK-6A (position 17/20 in Fig. 9) was measured by the proton recoil method, Li^6 and He^3 counters, and with the sandwich foil method. When the proton recoil method was used the reactor was subcritical (all absorber rods were inserted in the reactor) because the counting rates must to be low for this method. For measurements with the other methods the reactor was critical.

4.3.2 Results of the calculations

Three cross-section sets were used for the calculations, the MOXTOT- and NAPPMB cross- section set and the 208 groups set /12/. The data of the last set corres-

ponds to that of the KFK-SNEAK cross-section set /17/. The REMO correction was applied to the two 26-group sets in order to

a) have a better weighting spectrum

b) calculate better the influence of the resonances on the elastic removal cross-sections.

In the calculations the modified core configuration for the proton recoil measurements (absorber rods in) was taken into account. Fig. 17a - 17b show the experimental and calculated results and one observes that the 208 group calculations agree well with the measurements.

4.4 Reaction rate traverses

4.4.1 Axial direction

4.4.1.1 Experiments

a) Chamber measurements

The chamber measurements used the axial channel. The measurements were performed in the upper core half and in the upper axial breeder blanket. The distance between the measuring points was 1 cm in the core zone and in the blanket near the core boundary. In the remaining blanket zone, the distance was 3 cm. The statistical accuracy of the measurement was in the core- and inner blanket zone 0.3 %, in the outer blanket zone 0.7 %.

b) Foil measurements

Axial traverses were also measured with foils. The reaction rates could not be measured directly inside the fuel platelets. Therefore the foils were irra-

diated between the fuel and structural material platelets or in the structural material platelets of the core and blanket cells (see Fig. 5).

4.4.1.2 Calculations

The calculations of the axial reaction rate traverses were performed in the same manner as described in /1/ for SNEAK 2. The basic calculation was a two dimensional homogeneous diffusion calculation in RZ geometry with 26 groups and the MOXTOT cross section set. The results were corrected for transport- and heterogeneity effects. Tables 1b and 2b give the core compositions. For the foil measurements the heterogeneity effect was taken into account in a particular accurate manner since the foil reaction rates were calculated in the correct place in the heterogeneous cell, whereas the calculations for the chamber measurements were performed with cell averaged heterogeneous cross sections. The change of the spectra in the axial direction was also taken into account in the calculation of the heterogeneity corrected cross sections which were used for the calculation of the foil measurements: At different distances from the core mid-plane heterogeneity calculations were performed with the correct energy and position dependent B_m^2 which were obtained from a two dimensional diffusion calculation in RZ geometry.

The axial power distribution was determined using the measured relative rate distributions, the calculated central spectral indices σ_{f9}/σ_{f5} and σ_{f8}/σ_{f5} and the calculated corrections for higher Pu-isotopes. The results obtained from the measurements and calculations are given in Figs. 18 - 22.

4.4.2 Radial direction

4.4.2.1 Measurements

The fission rates of U-235, U-238 and Pu-239 were measured with chambers through the radial channel (position Y=19) as indicated in Fig. 9. The distance between successive points corresponds to 9 and 2 mesh intervals per element in the core and blanket, respectively. The pure statistical accuracy was 0.3 % in the core and 0.7 % in the blanket.

4.4.2.2 Calculations

The fission rate traverses were calculated using homogeneous diffusion theory in XY geometry with NAP-PMB group constants collapsed to 4 groups. The transport and condensation effects were estimated with one-dimensional calculations. The correction with regard to the heterogeneity of the cells was not performed. The B_z^2 values of all regions were taken from an RZ calculation.

The experimental and theoretical power density traverses were obtained by using the calculated spectral indices σ_{f9}/σ_{f5} and σ_{f8}/σ_{f5}, as given in Table 11.

4.4.2.3 Results and discussion

Fig. 24 shows the calculated and measured fission rates of the isotopes U^{235}, U^{238} and Pu^{239}, which are all normalized to unity in the center. With increasing distance from the core center an increasing underprediction of the experimental values is to be noticed. In the outer part of the blanket C/E values of 0.80 and 0.75 are obtained for the rates of Pu^{239} and U^{235} respectively. Experimental values for U^{238} are missing in the blanket.

The underprediction of the relative rates of U^{235} and Pu^{239} is reduced by about 10 % by using the MOXTOT-set.

The experimental and theoretical power density traverses are shown in Fig. 25. The comparison cannot be performed in the blanket due to the lack of experimental values. As indicated by the fission rate traverses the agreement is good (< 1 %) in the inner zone Z1A. It becomes worse when passing from Z1M to R1 in the outer part of which an underprediction of 10 % is reached.

4.5 The fine structure of the unit cell of the zone Z1A and the B_4C poisoned zone

The reaction rates were measured in two positions (position 1 and 2 in Fig. 5) in the unit cell of SNEAK-6A /6B and in the unit cell of the B_4C zone (see chapter 4.9.3). The measurements were done by the SNEAK experimental group and the group from MASURCA. The calculated fine structure is shown in Fig. 23. Table 10 gives the measured effects with their estimated errors and the calculated effects. The calculated values were obtained from a cell calculation with the code KAPER developed recently at Karlsruhe and with the MOXTOT cross-section set. The results represent average values over the entire platelet. The agreement between measured and calculated results is sufficiently good.

4.6 Reaction rate ratios

Fission ratios were measured by the SNEAK-group and the group from MASURCA in the configurations SNEAK-6A and SNEAK-6B. The measurements were calibrated with two absolute parallel plate fission chambers located

in the element 11/17 (see Fig. 9). During the measurements foils were located between the chambers to provide a calibration for fission ratio measurements with foils in the central cell. Table 11 gives the calculated and measured results. The calculated values were obtained from a two dimensional homogeneous diffusion calculation corrected for heterogeneity as described for the foil measurements in 4.4.1.2. These ratios were also measured in the B_4C poisoned zone. Table 11 gives also the results of this experiment.

4.7 Material worth determination

4.7.1 Experiments

The material worth measurements in SNEAK-6A and SNEAK-6B were performed with the pile oszillator (see /1/). The worth of fuel isotopes, absorber- and structural materials were measured in SNEAK-6A. To study the influence of the MASURCA buffer zone some of the more important samples were also measured in SNEAK-6B. In addition in SNEAK-6B an experiment was performed to measure the worth of sodium in two different arrangements of the unit cell. In the first arrangement the environment of the sodium platelet was fuel, in the second arrangement structural material was immediately adjacent to the sodium (see Fig. 4).

4.7.2 Calculations

The calculated results were obtained using the following methods:

1) one dimensional diffusion pertubation theory and homogeneous cross-sections with 26 groups in cylindrical geometry

2) the code KAPER which takes into account the heterogeneity of the probe and the environment.

All of the calculations were performed with the MOXTOT cross-section set, for comparison some calculations were repeated with the NAPPMB cross-section set. Table 12 gives the experimental and calculated results. One observes that the results of the material worth measurements in SNEAK-6A and SNEAK-6B agree well if the difference in β_{eff} for both cases is taken into account. (The difference in the normalization integrals is negligible.) The β_{eff} for SNEAK-6A and 6B were obtained from two dimensional diffusion theory calculations.

	SNEAK-6A	SNEAK-6B
β_{eff}	.00421	.00485

The ratio of the β_{eff} of SNEAK-6A to SNEAK-6B is 0.86. One finds approximately this factor if one compares a material worth of SNEAK-6A with the same of SNEAK-6B. In general the calculated results agree with the measured ones within 10 - 20 %. On the average one observers that the results calculated with the KAPER code fit the measured values better than the results of the one dimensional pertubation theory.

Table 13 gives the results of the sodium void measurements in the bunched cell configuration. It is seen that the calculation with the KAPER code reproduces the experimental results quite satisfactorily.

4.8 Sodium void measurements

4.8.1 Sodium void in axial direction

4.8.1.1 Description of the experiments and their results

In both assemblies SNEAK-6A and SNEAK-6B the sodium void effect was measured along the core axis, in zones which were enlarged stepwise from a size of 2 l to 9.5 l. In the four central elements in 3, 5, 7, 9 and 13 cells, and then over the full core height, the sodium platelets were replaced by empty steel cans. Fig. 3 shows the structure of the void cell and Table 3 gives the compositions. In another experiment the reactivity worth of sodium was measured in different axial positions using the pile oszillator. One sodium platelet was replaced by an empty steel can /1/.

4.8.1.2 Methods of calculation and results

The calculated results were obtained by the following methods.

1) one-dimensional diffusion perturbation theory with homogeneous and heterogeneous averaged cross-sections in slab geometry with 26 energy groups. The heterogeneous cross-sections were obtained from the ZERA code. The utilized radial group independent bucklings were from a two-dimensional diffusion calculation in R-Z geometry. In the case of one-dimensional calculations only the MOXTOT set was used.

2) two-dimensional diffusion perturbation theory. In the case of SNEAK-6A the 2-d calculations were performed with homogeneous cross-sections, twelve energy groups and the NAPPMB cross-section set,

while in the case of SNEAK-6B, the MOXTOT cross-section set, 26 energy groups and heterogeneous averaged cross-sections were used.

3) The influence of the REMO correction on the sodium void effect was studied by repeating one dimensional calculations with REMO corrected cross-sections.

The calculated results of the local sodium void effect were obtained by one dimensional diffusion pertubation calculations with heterogeneous averaged cross-sections from the MOXTOT cross-section set and homogeneous cross-sections from the NAPPMB cross-section set.
Fig. 26 shows the experimental and calculated results of the local sodium void effect, Table 14 gives the results of the axial sodium void effect as a function of the axial void height.

4.8.1.3 Discussion of the experimental and calculated results

In comparing the reactivities in the two assemblies the ratio of the β_{eff}'s and normalization integrals must be taken into account as was stated in 4.7.2. The ratio of reactivity worths should be $\rho(6B)/\rho(6A) = 0.86$. This is important for a comparison of the results. The following conclusions can be drawn from the experimental and calculated results:

1) The ratio of the measured void reactivities in SNEAK-6A and SNEAK-6B is the same as the calculated ratio of the reactivity scales. One can deduce that the buffer zone has no significant influence on the sodium void measurements, although the sodium void effect is certainly one of the most spectral sensitive effects. This means that on the axis of the

assembly the real and adjoint equilibrium spectrum is very well approximated, even in the absence of the buffer zone.

2) The influence of the REMO correction on the calculated effect is a reduction of about 10 %. The correction affects only the degradation term. The diffusion term in the calculations shows no influence as a result of the REMO correction.

3) One- and two-dimensional diffusion calculations are practically equivalent for the purpose of interpretation of the effect if good radial bucklings are used in the one-dimensional calculations.

4) The heterogeneity correction must always be used because it has a rather large influence on the calculated results.

4.8.2 Sodium void in radial direction

4.8.2.1 Experiments

In addition to the axial measurements of the sodium void effect measurements were also performed of the reactivity effect of a void of increasing radius. The voided zone, which extended over the entire core height was enlarged in four steps.

1. step the 4 central elements were voided
2. step 12 elements were voided
3. step 32 elements were voided
4. step 60 elements were voided

Fig. 14 shows the core cross-sections with the voided zones. The reactivity effects were measured with calibrated control rods. Calibration errors of 2.5 - 5 % and a reproducibility limit of about 0.05 ¢ must be taken into account.

4.8.2.2 Calculation methods and results

The calculated results were obtained with the following four methods:

1. One-dimensional diffusion and pertubation calculation

   The one-dimensional diffusion calculation in the axial direction was used to calculate the different void configurations, assuming a J_o dependence of the flux in the radial direction. This rather crude method of calculation is just used to test if larger void configurations of different radial extension can be calculated using the fundamental mode only in the radial direction. The results obtained with the MOXTOT-set and homogeneous and heterogeneous averaged cross-sections are shown in Table 15. Considering the simplicity of the calculational model the results are sufficiently accurate.

2. Two-dimensional diffusion pertubation theory

   The two-dimensional diffusion pertubation calculations in RZ geometry were carried out with 12 energy-groups (for the condensation scheme see Table 8), homogeneous cross-sections and the NAPPMB cross-section set. Table 17 gives the results.

3. Modified pertubation theory

   The largest and the smallest void configuration were calculated with a modified two-dimensional diffusion pertubation theory in RZ geometry and with heterogeneous cross-sections. The method used the unperturbed fluxes and the perturbed adjoint fluxes for the perturbation calculations. The MOXTOT cross-section set was used for the largest and the smallest void zone,

while the NAPPMB cross-section set was only used for the largest one. In Table 15 the experimental and calculated results are compared.

4. It is of interest to find the reactivity effect of large voids, which are important in the safety analysis of fast breeders by extrapolating the effect of small voids, which can be easily measured. In order to investigate whether this is possible, the effect of the axial void over the full height was extrapolated to the large radial voids using the expression:

$$\rho_R = A \int_0^R r\, dr\, J_o^2(B_r\, r) - C \int_0^R r\, dr\, J_1^2(B_r\, r)$$

where A und C are constants related to the effect of a void of 1 cm^2 cross-section along the axis, and to the radial diffusion coefficient. The results of the extrapolation are shown in Table 15 and compared to the actually measured values. The extrapolation gives good results for relative small voids, but overestimates the effect of large voids.

One observes that all four methods can be used for the interpretation of the measured results. The influence of the heterogeneity on the results is very large and there is some uncertainty in using SNEAK-results obtained in a platelet geometry to infer the void effect of a rodlet core of the SNR-type.

4.9 Material worth of Sodium and Boron in zones with a higher burn up

4.9.1 General remarks

For safety considerations of the SNR it is necessary to study the behaviour of the sodium void effect as a function of fuel burn up. In the SNEAK-6A core burn-up could be simulated.

a) by poisoning a central zone with higher Pu-isotopes (22.4 % Pu^{240}, normally 7.7 %)

b) by poisoning a central zone with B_4C, which simulates fission products.

4.9.2 The Pu-240 poisoning

In SNEAK-6A a central zone, with a higher Pu-240 enrichment was built by replacing the Pu-platelets (7.7 % Pu-240) normally used in the unit cell by platelets with 22.4 % Pu-240. This zone was surrounded by a buffer zone using different types of platelets but a similar integral composition to give a better equilibrium spectrum in the core center.

Fig. 13 shows the position and the radius of the zone. Fig. 6 shows the structure of the unit cell of the Pu-240 zone and that of the buffer zone. Table 7 gives the geometrical data of the zones and Table 4 gives the compositions used in the calculations.

In this zone the following effects were measured.

a) Reactivity effect by inserting the zone in the reactor
   α) the small zone
   β) the larger zone (Pu-240 zone with buffer zone)

b) The sodium void effect was measured in the reference core in the small and in the larger Pu-240 zone. In each case three central cells of the four central elements were voided (all sodium platelets in the cells were replaced by empty steel cans).

c) B_4C worth

To gain information on the behaviour of B_4C rods in a core with higher burn-up measurements of the B_4C worth were made in the reference core and in the zones with simulated higher burn-up, here in the Pu-240 zone. For this purpose in a central element, in three central cells, one sodium platelet was replaced by a B_4C-platelet. The contents of this platelet is B_4C-powder mixed with granulated aluminium.
The aluminium simulates the sodium of the replaced platelet. Fig. 8 shows the structure of the cells.

The effects were calculated with one-dimensional diffusion pertubation theory in spherical geometry and 26 groups, and with two-dimensional diffusion calculations in RZ geometry and 12 energy groups (condensation scheme see Table 8). Homogeneous cross-sections from the MOXTOT- and NAPPMB cross-section set were used for the calculations. The reference concentration of Pu 241 was used in most calculations. However, in the case of the small Pu 240 zone, a correction was applied for the decay of Pu 241, and build up of Am 241. The negative worth of Am 241 calculated with the cross-sections evaluated by Hinkelmann /19/, is about 60 % of the worth of Pu 239.
Table 16 shows the experimental and calculated results.

One observes that the B_4C-worth shows no modification in the two cases (reference core, large Pu-zone) and that the Na-void zone shows a small but constant modification when the size of the zone was enlarged. The conclusion of both effects is that an equilibrium spectra of the Pu-240 zone was not obtained and the size of this zone was not sufficient.

4.9.3 B_4C-poisoning

In the second simulation of the higher burn-up a central zone was poisoned with B_4C. The B_4C zone had 28 core elements and extended over the full core height. Fig. 7 shows the unit cell and Table 5 gives the utilized compositions. One sees that in the unit cell of the zone Z1A one sodium platelet was replaced by one B_4C-platelet.

In this zone the following effects were measured.

a) - the sodium void effect was measured in two configurations

   α) three central cells in the four central elements were voided

   β) nine cells in the four central elements were voided

b) - the worth of B_4C was measured in the same way as in the Pu-240 zone

The calculated results were obtained with one-dimensional diffusion pertubation theory in cylindrical geometry and two-dimensional diffusion pertubation theory in R-Z geometry. In the one-dimensional cal-

culations, heterogeneous averaged cross-sections were used, while in the two-dimensional case homogeneous cross-sections were used. The comparison of the experimental and calculated results is given in Table 17. When the B_4C-zone was built in the core, the uranium driver zone had to be enlarged to get the reactor critical. Therefore a new β_{eff} was computed. The new value is 5 % higher than in the reference core.

	reference	core with B_4C-zone
β_{eff}	421.10^{-5}	437.10^{-5}

The comparison of the measured results shows a significant increase of the sodium void worth in the case of the B_4C poisoning and a decrease of the B_4C-worth. The comparison of the measured and calculated effects gives a better agreement of the measured values

a) in the case of sodium void with the heterogeneous calculations with the MOXTOT cross-section set

b) in the case of the B_4C worth a better agreement with the calculations which used the NAPPMB cross-section set.

4.10 Cavities

In sodium cooled fast power reactors fuel-sodium reactions may occur and destroy part of the core. Cavity zones may be generated surrounded by regions containing an excess amount of fuel and structural materials. The reactivity of the system is influenced by this effect. The value of the reactivity change depends on the size and the position of the cavity as well as on the size of the condensed zone and the composition of fuel /16/.

In order to obtain informations on this effect reactivity experiments were performed in SNEAK-6A in a central and an off-center position. The cavities were built up stepwise:

1. sodium void in the cavity zone
2. partial sodium void in an adjacent region
3. PuO_2-UO_2 platelets shifted from the cavity into the adjacent zone
4. structural material shifted from the cavity into the condensed zone.

The geometry is shown in fig. 15 and fig. 16. More experimental details are given in chapter 2 of this report. Calculations were performed for the central position only. They are made rather difficult by the following reasons:

a) the small cavity volume (5 l) results in a small reactivity effect and requires high mathematical accuracy.

b) the shape of the cavity (large height, small diameter) prevents a transformation into spherical geometry. At least two-dimensional calculations are required.

c) the cavity region cannot be excluded from the rest of the system by suitable boundary conditions in diffusion calculations. Therefore the validity of diffusion theory is doubtful because the diffusion constants are very large within the cavity.

The total reactivity effect was investigated by two-dimensional transport calculations (TDC, S4-apprioximation, 4 energy groups) in r-z geometry using NAPPMB cross-sections. The effect of group collapsing (12 to 4 groups) was determined by r-z diffusion calculations (DIXY). Further extension of the number of groups up to 26 has negligible influence on reactivities.

The very small reactivity changes of the individual steps in the construction of the cavity were calculated by perturbation theory based on normal and adjoint 12-group-fluxes in r-z geometry (DIXY). The convergence criteria for the k_{eff} was 10^{-5}. The results are shown in Table 18.

In the central position the main part of the total effect is produced by sodium void. For these steps the agreement of experiments and perturbation-theory is satisfactory. The shifting of fuel and of structural material could not be calculated by applying that theory.

The results of 4 group transport calculations is reduced by a group collapsing correction from 14.9 ¢ to 7.2 ¢. The underestimate of the experimental value amounts to about 11 %.

Because of the difficulties mentioned above /a), b), c),/ and because of the large collapsing-correction with its methodical uncertainty (diffusion approximation) it seems impossible to draw from this investigation a general conclusion that could be applied to large cavities of interest for reactor safety considerations.

5. Assembly SNEAK-6D

The arrangement SNEAK-6D results from the arrangement SNEAK-6A by exchanging the zones Z1A (SNEAK platelets) and Z1M (MASURCA rodlets) and extending the zone Z1M over the total core height. The configuration SNEAK-6D was built according to a request by the MASURCA group which was particulary interested in repeating some of the central experiments of 6A inside a zone which is built with rodlets. Since the compositions of the platelet-zone Z1A and the rodlet-zone Z1M agree very well, discrepancies in identical experiments should be mainly the result of the different fuel geometry. The investigations on the configuration SNEAK-6D are described in detail in /18/. In the present report only two experiments are described which were of special interest in connection with SNEAK-6A and 6B.

5.1 Critical experiment

5.1.1 Experimental result

The measured k_{eff} with inserted shim- and control rods was

$$k_{eff}(exp.) = 1.00014$$

5.1.2 Methods and results of the k_{eff} calculations

The criticality of the SNEAK-6D core was calculated with the cross-section sets MOXTOT and NAPPMB. As a base for the final k_{eff} the result of a homogeneous, two-dimensional, 26-groups diffusion calculation in R-Z geometry was used. The resulting k_{eff}-value was corrected for anisotropy (S_8-correction), heterogeneity and the non-circular shape of the core. The

cell model for the heterogeneity correction of the Z1M- and MASURCA breeder blanket zone was cylindrical and consists of two zones with fuel in the center. The dimensions and compositions of these unit cells are shown in Fig. 27. Furthermore the k_{eff}-value of the base calculation was REMO-corrected. All corrections- except the cylinderisation correction- were found by means of 1-d, 26 groups calculations. The bucklings used were group- and composition dependent and were derived from the 2-d diffusion calculation.

The results of the criticality calculations are shown in Table 19.

5.2 Sodium void in axial direction

5.2.1 Description of the experiments and their results

Similar to the procedure in SNEAK-6A and 6B the sodium was first removed from the four central elements in four steps. Beginning in the core center the height of the voided zones were 10.2 cm, 50.8 cm, 71.1 cm and 91.45 cm (full core height). Table 20 shows the experimental results.

5.2.2 Methods and results of the calculations and comparison with the experimental results

All sodium-void calculations were performed using 2 d pertubation theory in (R-Z) geometry and heterogeneity corrected MOXTOT cross-sections. In Table 19 the experimental and calculated results are compared. It is interesting to notice that the calculated sodium void effect for the total height is in agreement with the experimental one within 5 %.

6. Comparison of results from SNEAK 6A/6B and SNEAK-6D and conclusions

6.1 Comparison of the k_{eff} results

Table 21 shows all results of the k_{eff} calculations of the three core configurations. One observes that the MOXTOT-set gives for these mixed core configurations better results than the NAPPMB-set. It appears that the prediction of k_{eff} for such a core-type using the MOXTOT-set in general is correct within $\pm$ 5 % in k_{eff}. The best NAPPMB-set calculations (SNEAK-6D) underestimates k_{eff} and shows a discrepancy of 1 %.

6.2 Comparison of sodium void experiments in SNEAK-6A, SNEAK-6B and SNEAK-6D

Fig. 28 shows the measured reactivity changes of SNEAK-6A, SNEAK-6B and SNEAK-6D caused by voiding the four central elements up to a height H. The results of SNEAK-6A, 6B and 6D are normalized to each other considering the different worths of β_{eff}. The figure also shows corresponding calculational results for the core SNEAK-6D using quasihomogeneous and heterogeneity corrected cross-sections. One observes that calculation and experiment agree well if heterogeneity-corrected cross-sections are used.

A comparison of the maximum value of the sodium void effect and of its decrease towards the core edge for the different configuration, shows that the maximum value is smaller in the case of SNEAK-6D, the decrease is steeper and the void effect of the full

height is negative. These three effects can be explained by the different geometry of the fuel and structural material in the case of SNEAK-6D. The rodlet structure of the sodium material and the empty channel structure of the voided zone causes a large streaming effect in the axial direction and therefore an increased diffusion term of the void effect. Efforts are now underway to get a better understanding of the behaviour of the Na-void effect in systems of different heterogeneity.

ACKNOWLEDGEMENT

The authors gratefully acknowledge the valuable help from R. Kiesel, M. Mäule and H. Fries as well as the steady cooperation of the SNEAK operation group.

References

/ 1 / F. Helm et al.
Physics Investigations of Sodium-Cooled Fast Reactors SNEAK-Assembly 2,
KFK 1399 d, June 1971

/ 2 / R. Böhme et al.
Messung von Reaktionsraten im Schnellen Nullleistungsreaktor SNEAK
ATW Juli 1971, p. 360

/ 3 / M. Müller
Messung von Neutronenspektren im Energiebereich 1 eV bis 10 keV mit Hilfe der Sandwichtechnik
KFK 1233, July 1970

/ 4 / H. Bluhm and D. Stegemann
Theoretical and Experimental Investigations for an Improved Application of the Li^6 Semiconductor Sandwich Spectrometer
Nucl. Inst. and Methods 70 1969, No. 2 p.141-150

/ 5 / H. Bluhm
2. Vierteljahresbericht 1970 PSB
KFK 1270/2, p. 121-1

/ 6 / H. Bluhm et al.
Poc. BNES-Conf. Fast Reactor Physics,
London 1969, p. 61

/ 7 / Messung und Berechnung schneller Reaktorspektren zur Prüfung von Gruppensätzen
Reaktortagung Bonn 1971, 30. März - 2. April

/ 8 / KFK 770 H. Huschke
Gruppenkonstanten für dampf- und natriumgekühlte schnelle Reaktoren (26 Gruppen)

/ 9 / KFK-969 E. Kiefhaber, J.J. Schmidt
Evaluation of Fast Critic. Exp.
Using Recent Methods and Data

/ 10 / C. Günther & W. Kinnebrock
SNOW, ein zweidimensionales SN-Programm zur Lösung der Neutronen-Transportgleichung in Platte- und Zylindergeometrie
Unveröffentlicht, 1971

/ 11 / KFK-1361 W. Kinnebrock
Strategien zur Beschleunigung zweidimensionaler SN-Verfahren mit Hilfe der Grobgittertechnik

/ 12 / H. Huschke, D. Sanitz, D. Woll & J. Braun
KFK 1270/2
Projekt Schneller Brüter, 2. Vierteljahres-bericht 1970
1222.2: Zur Berechnung des Neutronenflusses in sehr vielen (208) Energiegruppen

/ 13 / P. Mc Grath & E.A. Fischer
KFK-1557
Calculation of Heterog Fluxes Reaction Rates and Reactiv. Worths in the Plate Structure of zero Power Fast Critical Assemblies

/ 14 / KFK-743 D. Wintzer
Zur Berechnung von Heterogenitätseff. in period. Zellstrukturen therm. und schneller Kernreaktoren

/ 15 / KFK-1036 W.J. Oosterkamp
The Measurement and Calc. of the Reactiv. Worth of Samples in Fast Heterog. Zero Power Reactors

/ 16 / DAtF 1971 Reaktortagung Bonn, Tagungsbericht
A. Stojadinović et al.

/ 17 / KFK 628 H. Bachmann, H. Husche, E. Kiefhaber et al.
The Group Cross-Section Set KFK-SNEAK Preparation and Results

/ 18 / CEN/KFK-1581 Plum et al.
to be published soon

/ 19 / KFK-1186 Hinkelmann
Microscop. Neutron Nuclear Data and 5 Group Cross Sections for Actinides
U-232, U-234, U-236, U-237, Np-237, Np-238, Pu-236, Pu-238, Am-241, Cm-242

Table 1a Atomic compositions (10^{22} at/cm^3) SNEAK-6A (used for the k_{eff} calculations)

Zones / Isotopes	Core Zones					Blanket Zones		
	Z1A'	Z1A	Z1MAS	R1 above and below Z1MAS	R1	Axial Breeder Blanket for Z1A' and Z1A	Axial Breeder Blanket for Z1MAS and R1	Rad. Blanket
Al	0.00037	0.03193	0.04908	0.83098	0.84053	0.29507	1.23579	0.51550
C	0.00492	0.01522	0.01841	0.61574	0.63017	0.00471	0.00430	
Cr	0.30822	0.30792	0.33170	0.34118	0.34239	0.25497	0.28466	
Fe	1.19122	1.18622	1.23929	1.22489	1.22408	0.90300	1.01055	
Mn	0.01471	0.01505	0.01000	0.02269	0.02263	0.01271	0.01859	0.00004
Na	0.84832	0.82438	0.84374	0.26188	0.28626	0.64446	0.02464	
Ni	0.22735	0.22407	0.16895	0.19127	0.18984	0.14319	0.14438	0.04122
O	1.20000	1.18724	1.14325	0.57354	0.51683	1.38478	1.35988	
Pu-239	0.12112	0.11477	0.11096	0.00630				
Pu-240	0.01088	0.01031	0.01022	0.00057				
Pu-241	0.00099	0.00094	0.00097	0.00005				
Pu-242	0.00005	0.00005	0.00012					
Si	0.01528	0.01529	0.00587	0.01994	0.02014	0.01486	0.02307	0.00115
Ti	0.00092	0.00112	0.00042	0.00404	0.00403	0.00013	0.00226	0.00006
U-235	0.00464	0.01424	0.01726	0.18760	0.18929	0.00499	0.00516	0.01624
U-238	0.67889	0.68259	0.60916	0.66421	0.66291	0.68791	0.75683	3.99400

Table 1b

Atomic compositions (10^{22} at/cm^3) SNEAK-6A

Zones / Isotopes	Compositions used in calculations of reaction rate distributions				Composition of SNEAK-Control Rods
	Z1A	Z1MAS	R1	Blanket Zones	All Zones
Al	0.00037		0.85301		0.58877
C	0.00494	0.00135	0.65227		0.20443
Cr	0.30881	0.33547	0.34669		0.30255
Fe	1.19161	1.25480	1.23859		1.09661
Mn	0.01478	0.00874	0.02284		0.02117
Na	0.85517	0.88556	0.27703		0.39720
Ni	0.22677	0.17644	0.19210	The k_{eff}-	0.16495
O	1.19981	1.15970	0.48412	compositions	0.94442
Pu-239	0.12154	0.12104		(see Table 1a)	
Pu-240	0.01092	0.01116		were used	
Pu-241	0.00094	0.00106			
Pu-242	0.00005	0.00013			
Si	0.01529	0.00456	0.02051		0.01550
Ti	0.00092		0.00403		0.00471
U-235	0.00464	0.01603	0.18774		0.18824
U-238	0.67427	0.59296	0.65159		0.75117

Table 2a Atomic compositions (10^{22} at/cm^3) SNEAK-6B (used for the k_{eff} calculations)

Isotopes	Core Zones			Blanket Zones		
	Z1A'	Z1A	R1	Axial Breeder Blanket for Z1A' and Z1A	Axial Breeder Blanket for R1	Radial Blanket
Al	0.00037	0.03193	0.84769	0.29507	1.23954	0.31168
C	0.00492	0.01522	0.62009	0.00471	0.00433	0.00054
Cr	0.30822	0.30792	0.34061	0.25497	0.28344	0.04445
Fe	1.19082	1.18622	1.21806	0.90300	1.02034	0.15637
Mn	0.01471	0.01505	0.02263	0.01271	0.01981	0.00284
Na	0.84832	0.82438	0.28552	0.64446		
Ni	0.22735	0.22407	0.18976	0.14319	0.14482	0.06385
O	1.20000	1.18724	0.51871	1.38478	1.34171	
Pu-239	0.12112	0.11477				
Pu-240	0.01088	0.01031				
Pu-241	0.00099	0.00094				
Pu-242	0.00005	0.00005				
Si	0.01528	0.01529	0.02013	0.01486	0.02347	0.00249
Ti	0.00092	0.00112	0.00402	0.00013	0.00232	0.00004
U-235	0.00464	0.01424	0.18789	0.00499	0.00520	0.01624
U-238	0.67889	0.68259	0.65919	0.68791	0.75668	3.99400

Table 2b

Atomic compositions SNEAK-6B

1. Compositions used in calculations of reaction rate distribution.

   These compositions are the same as in SNEAK-6A (see Table 1b).

2. The compositions of the SNEAK-Control Rods are the same as in SNEAK-6A (see Table 1b).

Table 3 Atomic compositions (10^{22} at/cm^3) for the voided zones in SNEAK-6A/6B

Isotopes	
Al	0.00037
C	0.00491
Cr	0.30650
Fe	1.18313
Mn	0.01463
Ni	0.22782
O	1.20016
Pu-239	0.12158
Pu-240	0.01092
Pu-241	0.00099
Pu-242	0.00005
Si	0.01544
Ti	0.00092
U-235	0.00438
U-238	0.64187

Table 4 Atomic compositions (10^{22} at/cm^3) of the Pu-240 Zone in SNEAK-6A

Isotopes	Pu-240 Zone	Pu-240 Buffer Zone
Al		0.00059
C	0.00402	0.00487
Cr	0.30896	0.30010
Fe	1.19236	1.23394
Mn	0.01479	0.01509
Na	0.85559	0.85498
Ni	0.22807	0.23213
O	1.20354	1.21871
Pu-239	0.11700	0.11539
Pu-240	0.03603	0.03010
Pu-241	0.00636	0.00981
Pu-242	0.00143	0.00228
Si	0.01530	0.01605
Ti	0.00092	0.00092
U-235	0.00439	0.00447
U-238	0.64909	0.66067

Table 5 Atomic compositions (10^{22} at/cm^3) of the B_4C poisoned zone in SNEAK-6A

Isotopes	
Al	0.14180
B-10	0.03591
B-11	0.13385
C	0.04659
Cr	0.30827
Fe	1.19026
Mn	0.01475
Na	0.68396
Ni	0.22661
O	1.19949
Pu-239	0.12151
Pu-240	0.01091
Pu-241	0.00099
Pu-242	0.00005
Si	0.01561
Ti	0.00092
U-235	0.00461
U-238	0.67409

Table 6 Impurities in the chamber deposits

Fission Chamber		FC4 20th Century Electronics Ø = 6.35 mm		French Chambers Ø = 8 mm	
Isotope	Type	Exact isotope contents	Deposit	Type	Exact isotope contents
U-235	TI 500	U-235 93 % U-238 5.5 % U-234 1.25% U-236 0.25%	U_3O_8 1000 µg/cm^2 4 cm^2	552 C	U-235 99.87 ±0.03 % U-238 0.053±0.01 % U-234 0.036±0.008% U-236 0.039±0.00 %
U-238	UD 73	U-238 99.956% U-235 0.044%	U_3O_8 1000 µg/cm^2 4 cm^2	871 C	U-238 99.98% U-235 0.02 ±0.003%
Pu-239	TI 536	Pu-239 99 % Pu-240 1 %	PuO_2 300 µg/cm^2 4 cm^2	961 C	Pu-239 98.37% Pu-240 1.59% Pu-241 0.03%
Np-237	UI 370	Np-237 99.9 % Pu-239 0.1 %	NpO_2 300 µg/cm^2 4 cm^2	772 C	Np-237 99.9 % Pu-239 0.1 %

Table 7 Geometry of the Pu-240 zone in SNEAK-6A

	Equivalent Radius	Height
Pu-240 zone	11.06 cm	18.37 cm
Pu-240 axial buffer zone		6.12 cm
Pu-240 radial buffer zone	14.72 cm	30.61 cm

Table 8 The 12 groups condensation scheme

ABN - 26 groups	Broad group no.
1-4	1
5	2
6	3
7	4
8	5
9	6
10	7
11	8
12	9
13	10
14	11
15-26	12

Table 9 Results of the k_{eff} calculations for SNEAK-6A/6B

Cross section set	MOXTOT		NAPPMB	
Assembly	6A	6B	6A	6B
2-d hom. diffusion calculation	.9887	.9965	.9887[2)]	.9732
1-d difference calculation MOXTOT - NAPPMB			-.0179	
Correction for cylindrisation	-.0016	-.0019	-.0016[2)]	-.0019[2)]
REMO correction	+.0038	-.0026	+.0093	+.0069
Heterogeneity correction	+.0027	+.0012	+.0034	+.0016
Transport (S_8)[1)] correction	+.0041	+.0041	+.0041[2)]	+.0041[2)]
Final results	0.9977	1.0025	0.9860	0.9839

1) Correction in axial and radial direction

2) This result is taken from MOXTOT set

Table 10

Fine structure of the reaction rates and the reaction rate ratios in the unit cell of SNEAK-6A/6D and in the unit cell of the B_4C zone

$$\frac{R\ (Pos.\ 2) - R\ (Pos.\ 1)}{R\ (Pos.\ 1)} \quad \text{in } \%$$

		6A and 6B cell	Calculation with code KAPER	Unit cell of the B_4C poisoned zone in SNEAK-6A	Calculation with code KAPER
Measurements of SNEAK-group	R_f^{28}	3.8±1	≈4%	5.0±1	≈5%
	R_f^{25}	0 ± 1	≈0%	0 ± 1	≈0%
	R_c^{28}	3.0±1	1%-4%	4.3±1	1%-5%
Measurements of Cadarache-group	$\sigma_f^{28}/\sigma_f^{25}$	4.0±1	≈4%		
	$\sigma_c^{28}/\sigma_c^{25}$	3.3±1	1%-4%		

Table 11 Reaction rate ratios of SNEAK-6A/6B

	SNEAK-6A						SNEAK-6B	
	Experiment				Calculations 2d HET	C/E	Experimentell	Calculations 2d HET
	group	result	error					
			max.error	geom.addition				
σ_f^8/σ_f^5	GfK	.0276	5%	2.5%	.0242	.877	.0284	.0242
reference core	Cadarache	.0276						
σ_f^8/σ_f^5 B_4C poisoned zone	GfK	.0307			.0257	.84		
σ_f^9/σ_f^5	GfK	.975	4%	2.1%	.902	.925		
σ_c^8/σ_f^5	GfK	.128	5.5%	2.7%-3.4%	.134	1.05		
σ_c^8/σ_f^8					5.512	1.20		
σ_c^8/σ_f^9					.147			

Table 12 Material worth in SNEAK-6A/6B

Isotopes	SNEAK-6A					SNEAK-6B		SNEAK-6B / SNEAK-6A
	Weight ⌶g⌶	Experiment μ$/g	Calculations C/E			Experiment μ$/g	Calculations C/E	
			Diff. 1d MOXTOT	KAPER MOXTOT	Diff. Perturb. 2d NAPPMB		Diff. 1d MOXTOT	Experiment
U-235	3.3	512±10	1.22	1.19	1.24	466±10	1.13	.91
U-238	62.	-33.2±.5	1.25	1.19	1.34	-28.3±.4	1.24	.855
Pu-239	4.	740±7	1.05	1.03	1.14	645±8	1.01	.87
Pu-240	2.7	107±10	.99	.97	.35			
SS	17.	-27.2±2	.89	.90	.93			
Fe_2O_3	3.	-10.±10	3.1	3.1				
B_4C	6.	-1720±5	1.11	1.04	1.07	-1480±7	1.09	.86
Eu_2O_3	4.	-705±8	.91	.88	.85[1)]			
Ta	220.	-143±.2	1.90	1.07	1.81			
Na	30.	-31.3	1.14	1.38	1.23	-27.1±2	1.13	.865

Estimated error of the measurements: 5%

1) With new ENDF/B data there is a better agreement: .93

Table 13 Na-void in SNEAK-6B (μ$/g)

	Experiment	KAPER
Na between fuel	-25.5	-31.33
Na between structural materials	-19.0	-23.7
Ratio $\frac{\text{pos. between fuel}}{\text{pos. between structural materials}}$	1.342	1.322

Estimated error of the measurements: 5%

Table 14

Reactivity worth of the sodium void effect in axial direction in SNEAK-6A/6B

Voided zone		SNEAK-6A (β_{eff}: $421 \cdot 10^{-5}$)					SNEAK-6B (β_{eff}: $485 \cdot 10^{-5}$)		Comparison of the experimental results SNEAK-6B/6A
			Calculation [¢]						
			MOXTOT			NAPPMB			
voided height [cm]	g Na removed	Experiment [¢]	1d HOM	1d HET	1d REMO HOM	2d HOM 12 groups	Experiment [¢]	Calculation [¢] 2d 26 groups, HET MOXTOT set	
18.36	706	2.32	2.73	2.31	2.36	2.72	2.0	1.48	.86
30.62	1178	3.58	4.23	3.59	3.62	4.27			
42.86	1649	4.62	5.23	4.40	4.55	5.29	3.9	3.75	.84
55.10	2120	5.00	5.63	4.59	4.86	5.65	4.3	3.96	.86
79.60	3063	4.24	4.52	3.09		4.63			
full height	3440	3.10			2.52		2.65	1.88	.85

Estimated error of the measurements: 5%

Table 15 Results of the radial void measurements (β_{eff}: $421 \cdot 10^{-5}$)

Step No.	Elements	Equivalent radius [cm]	Results of the experiment	Calculation C/E						
				1. method 1d MOXTOT		2. method 2d NAPPMB	3. method modified 2d perturbation			4. method extrapolation
				HOM	HET	HOM	MOXTOT HET	NAPPMB HOM	NAPPMB HET	MOXTOT
1	4	6.14	3.1 ¢	1.21	.77	1.07	.68			1.00
2	12	10.63	8.6 ¢	1.24	.76	1.11				1.03
3	28	17.4	19.6 ¢	1.27	.73	1.08				1.06
4	60	23.8	25.8 ¢	1.46	.70	1.12	.82	1.69	1.11	1.21

Estimated error of the measurements: 5%

Table 16 Results of the Pu^{240} experiment in SNEAK-6A (β_{eff}: $421 \cdot 10^{-5}$)

Configuration	Experiment			Experimental results Total effect [¢]	Calculation	
		Weight of Na removed or B_4C added			1d HOM (spherical geom.) 26 groups MOXTOT set Total effect [¢]	2d HOM 12 groups NAPPMB set Total effect [¢]
		Na removed [g]	B_4C added [g]			
Reference Core	Na-void	706		2.32	2.61	2.72
	B_4C worth		-21.01	-3.68	-4.19	
Small Pu^{240} zone	Inserting of this zone			12.1	17.7[a)] 14.1[b)]	16.56[a) 1)] 13.0[b) 1)]
	Na-void	706		2.50	2.75	
Large Pu^{240} zone	Inserting of this zone			77.1	94.5[a)]	
	Na-void	706		2.88	2.84	3.01[1)]
	B_4C worth		-21.01	-3.66	-4.0	-4.07[1)]

Estimated error of the measurements: 5%

a) The reference concentration of Pu^{241} was used

b) Corrected for the decay of Pu^{241} and build up of Am^{241}

1) MOXTOT set was used

Table 17 Results of the measurements in the B_4C-zone

Configuration	Experiment			Experimental results		Calculation			
		Weight of Na removed or B_4C added [g]		Total effect [¢]	effect/g [µ$/g]	1d HET 26 groups MOXTOT		2d HOM 12 groups NAPPMB	
		Na removed	B_4C added			Total effect [¢]	Effect/g [µ$/g]	Total effect [¢]	Effect/g [µ$/g]
Reference core $\beta_{eff} = 421 \cdot 10^{-5}$	Na worth (12 cells voided)	706		2.32	32.86	2.31	32.72	2.72	38.53
	B_4C worth		21.06	-3.68	-1751.5	-4.19[1)]	-1994.3		
B_4C zone $\beta_{eff} = 437 \cdot 10^{-5}$	Na worth 12 cells voided	566		2.66±.01	47.00	2.94	51.94	3.03	53.53
	Na worth 36 cells voided	1697		6.04±.06	35.95	6.66	39.24	6.87	40.48
	B_4C worth		21.6	-2.64	-1222.2	-3.18	-1472.2	-2.76	-1277.8

1) From the 1d HOM calculations from Table 10

Estimated error of the measurements: 5%

Table 18 Reactivity worths for the cavities in SNEAK-6A ¢

($\beta_{eff} = 4.17 \cdot 10^{-3}$)

Step	Central position					Off center
	Transport (4g)	Diffusion (4g)	Diffusion (12g)	Perturbation (12g)	Experiment	Experiment
1				5.3	4.6	1.4
2				2.6	2.6	0.7
3				(-12.6)	-0.8	-1.1
4				(-36)	1.7	-1.9
Total	14.9	6.5	-1.2	(-40.7)	8.1	-0.9
Corrected theoretical result					7.2	

Table 19 Results of the k_{eff} calculations for SNEAK-6D

	Cross section set	
	MOXTOT	NAPPMB
2d hom. diffusion calculation	.9866	.9696
Correction for cylindrisation	-0.0025	-0.0025[1)]
REMO correction	+0.0037	+0.0085
Heterogeneity correction	+0.0091	+0.0098
Transport (S_8) correction	+0.0046	+0.0046[1)]
Final result	1.0015	0.9900

1) This result is taken from MOXTOT set

Table 20 Reactivity worth of the sodium void effect in axial direction in SNEAK-6D

(β_{eff}: 397. · 10^{-5})

Voided height [cm]	Experiment [¢]	Calculation 2d HET MOXTOT [¢]	Calculation / Experiment
10.2	+ .94	1.03	1.10
50.8	+2.97	2.95	.99
71.1	1.84	1.63	.89
full height	-1.18	-1.24	1.05

Estimated error of the measurements: 5%

Table 21

Comparison of k_{eff}-calculation results of the assemblies SNEAK-6A, SNEAK-6B and SNEAK-6D

Calculation methods	SNEAK - assemblies					
	SNEAK-6A		SNEAK-6B		SNEAK-6D	
	MOXTOT set	NAPPMB set	MOXTOT set	NAPPMB set	MOXTOT set	NAPPMB set
2d homogeneous diffusion calculation	.9887	.9708[1)]	.9965	.9732	.9866	.9696
Correction for cylindrisation	-.0016	-.0016[2)]	-.0019	-.0019[2)]	.0025	-.0025[2)]
REMO correction	+.0038	+.0093	+.0026	+.0069	+.0037	+.0085
Heterogeneity correction	+.0027	+.0034	+.0012	+.0016	+.0091	+.0098
Transport (S_8) correction	+.0041	+.0041[2)]	+.0041	+.0041[2)]	+.0046	+.0046[2)]
Final result	.9977	.9860	1.0025	.9839	1.0015	.9900

1) This result is taken from MOXTOT set corrected with 1d difference calculation MOXTOT-NAPPMB

2) This result is taken from MOXTOT set

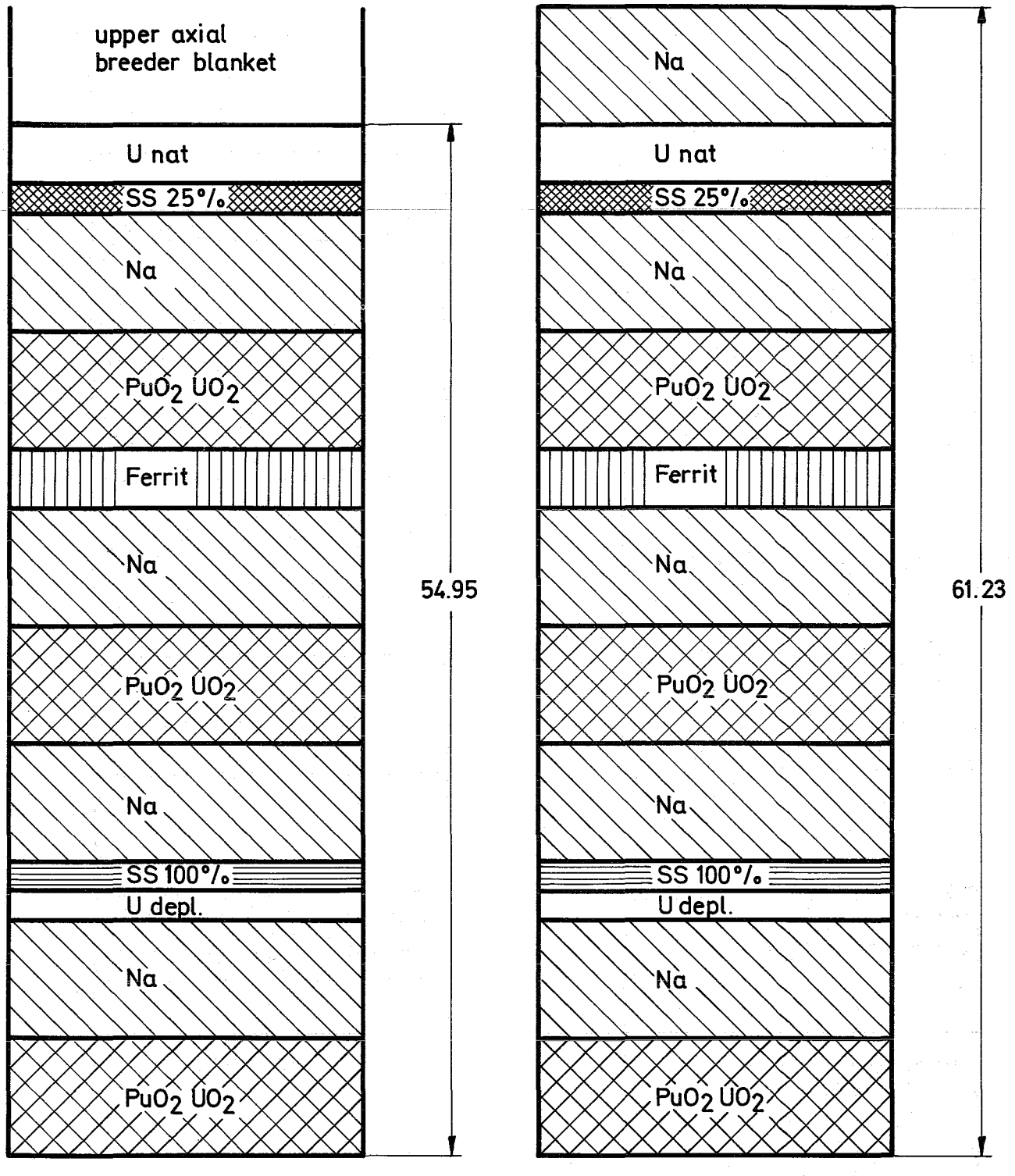

upper rest cell

normal cell

Fig. 1a Cells of the Zone Z1A

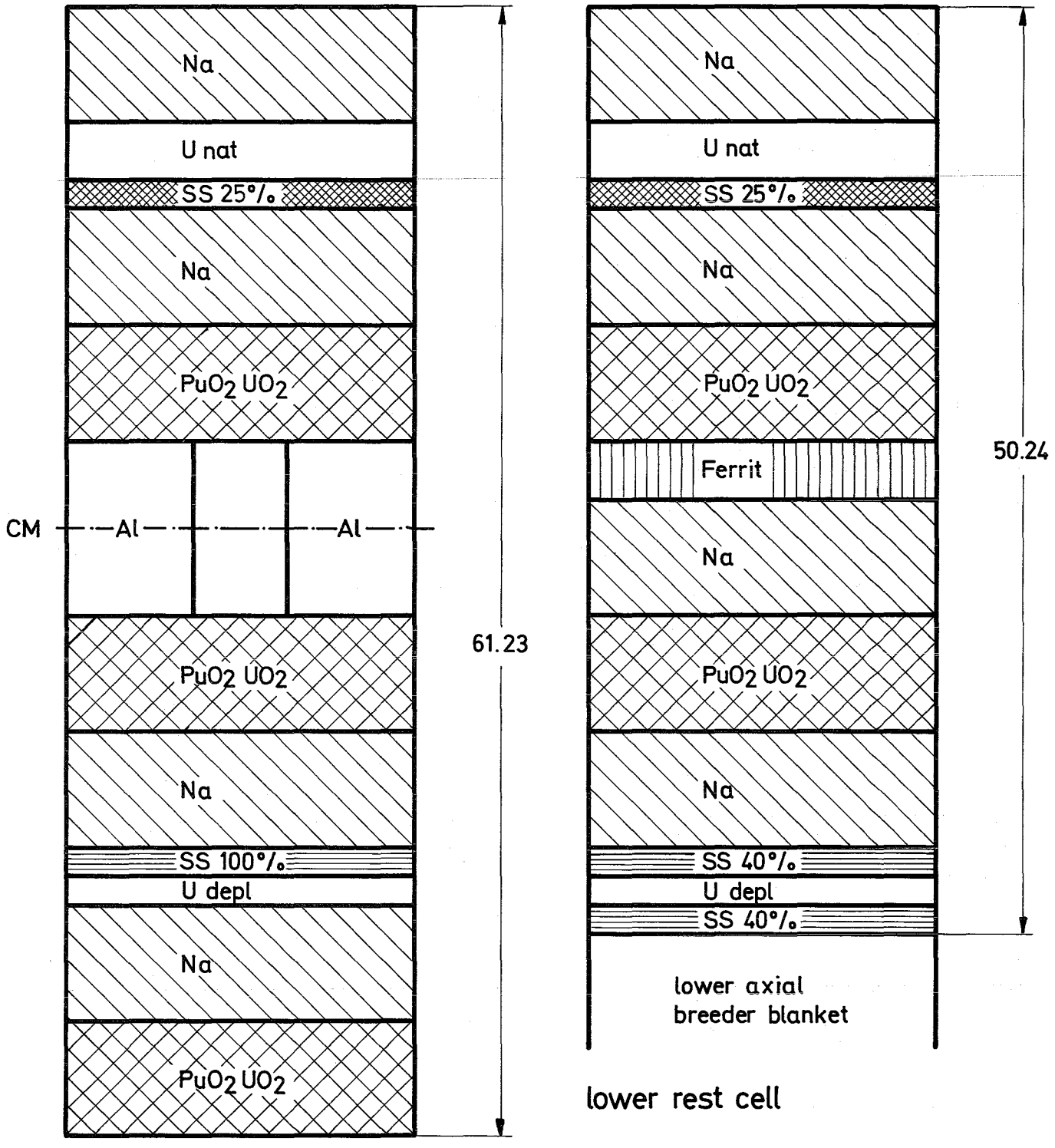

Fig. 1b Cells of the Zone Z1 A

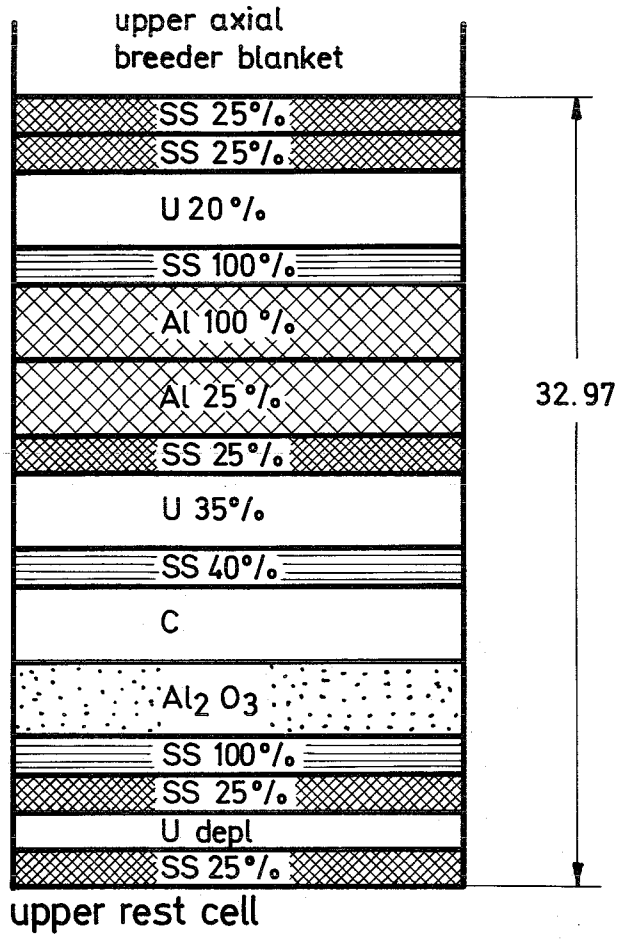

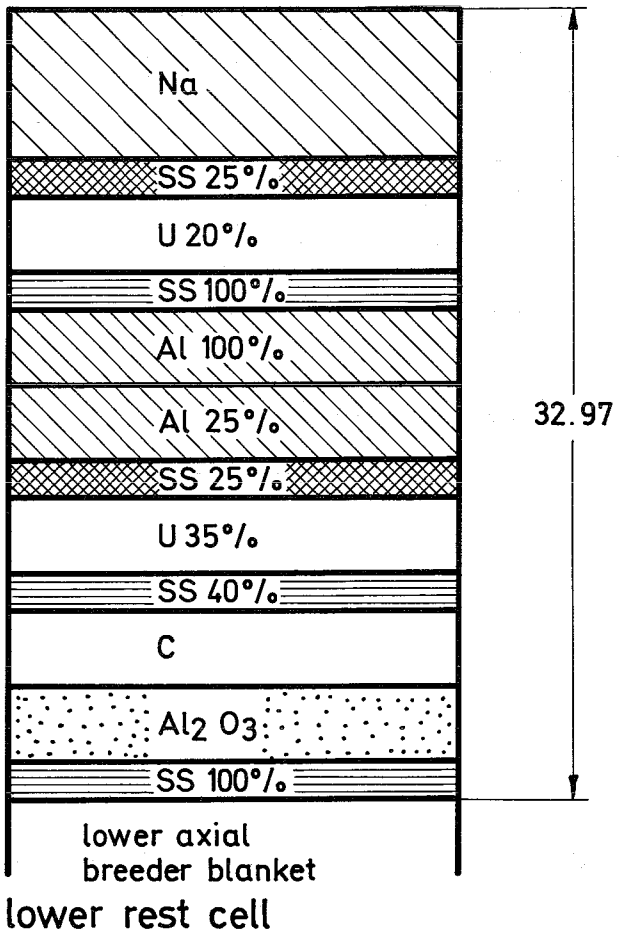

Fig. 1c Rest Cells of the Zone Z1 MAS.

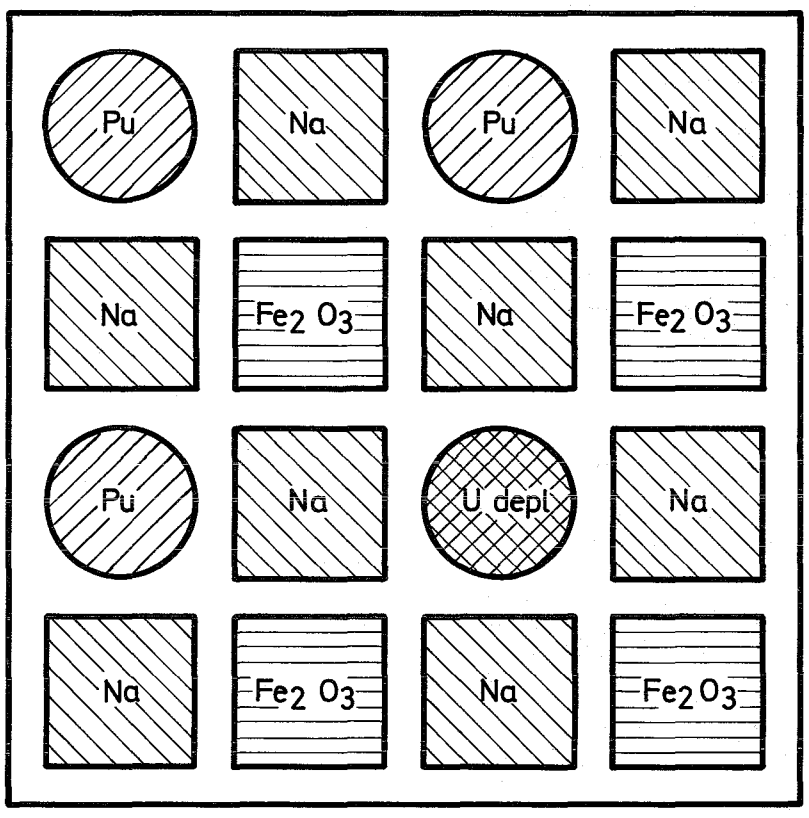

Cross section normal cell zone Z1 MAS.

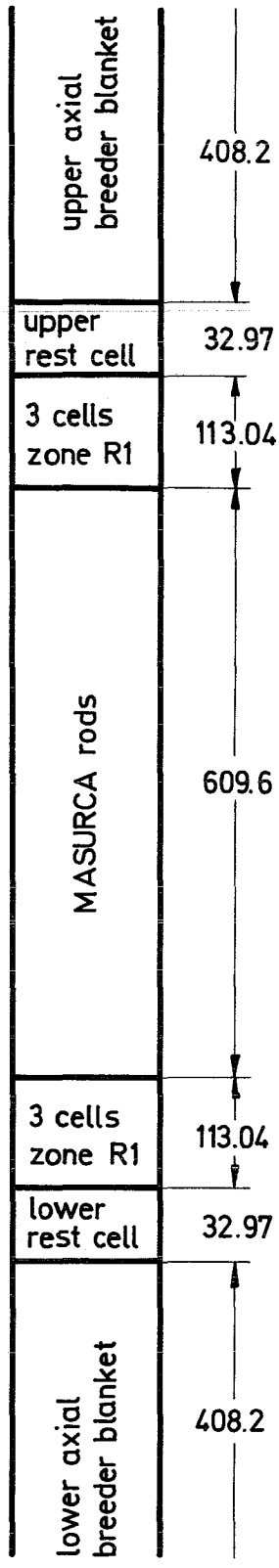

Fig. 1d Loading Schemes of Elements in the Zone Z1 MAS.

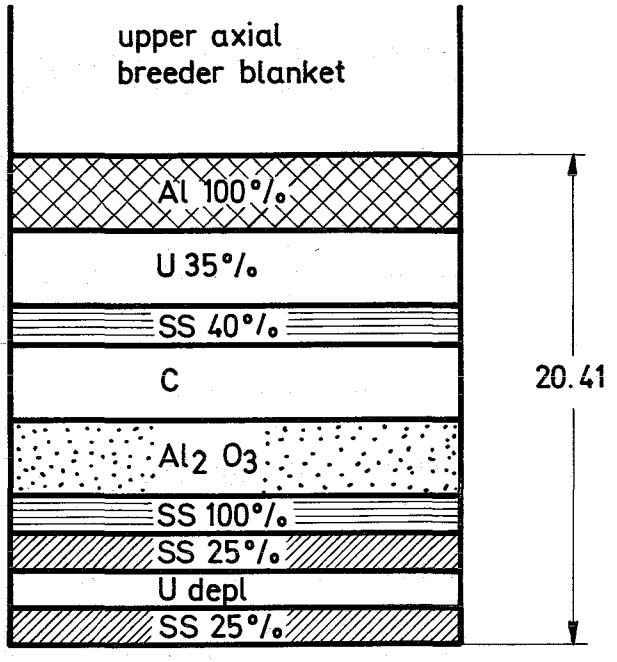

upper rest cell

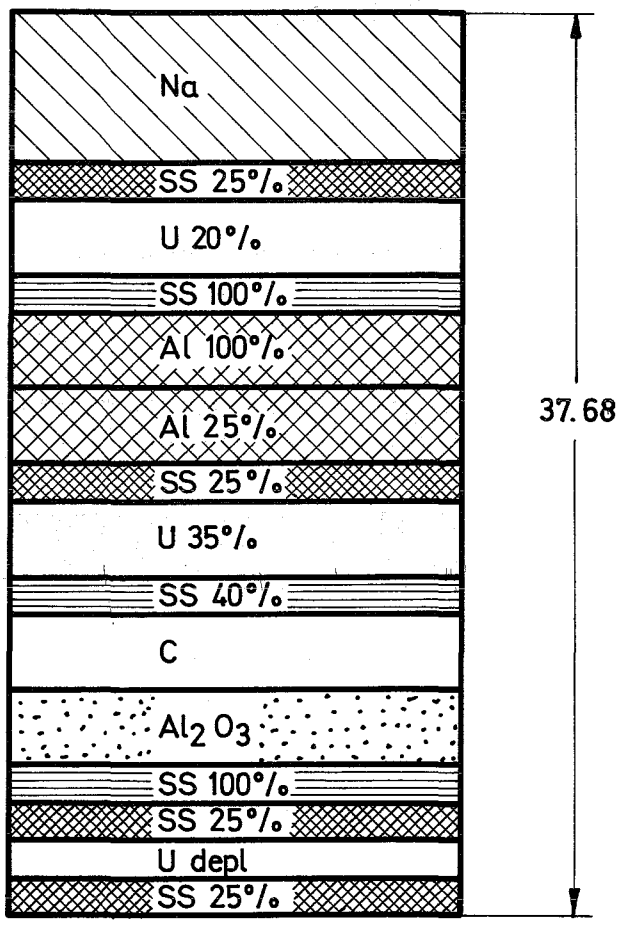

normal cell

Fig. 1e Cells of the Zone R1

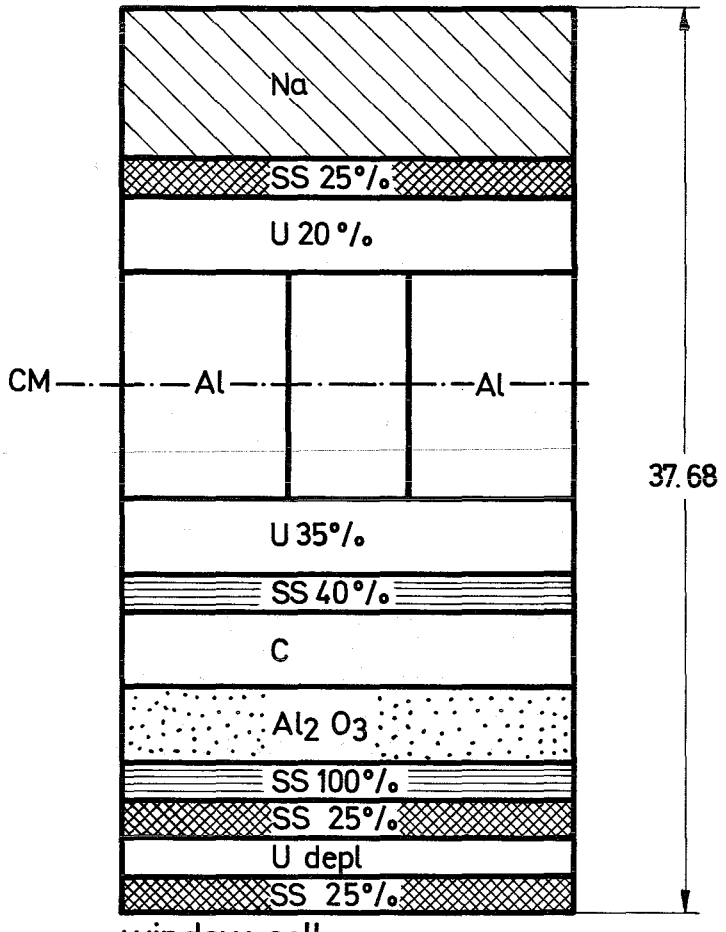

window cell

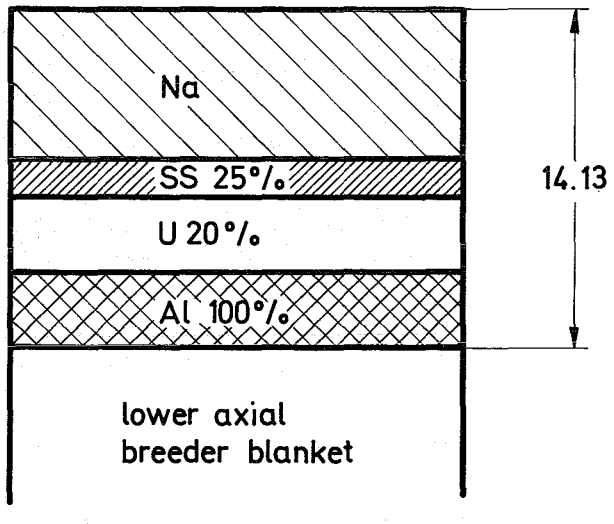

lower rest cell

Fig. 1f Cells of the Zone R1

Cell for Breeder Blanket in the zone Z1 A

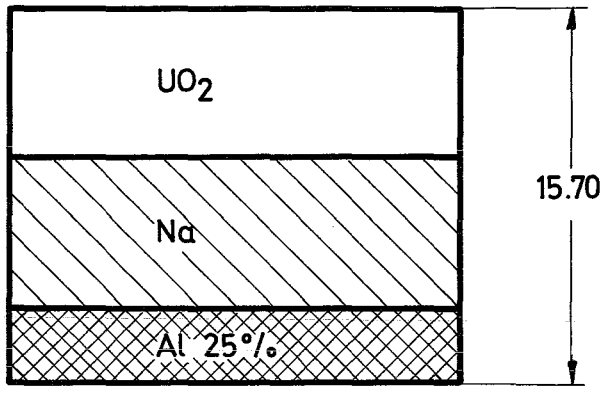

Cell for Breeder Blanket in the zone Z1 MAS. and R1

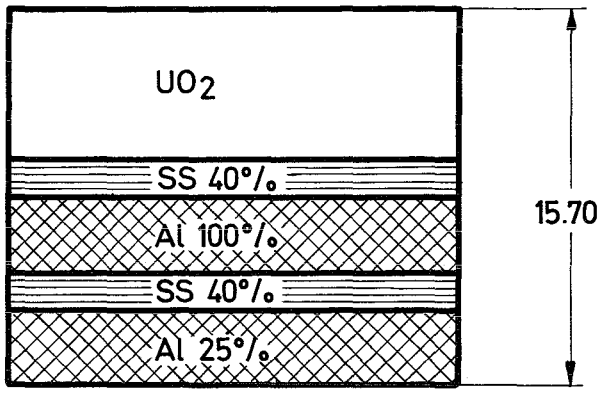

Cell for Breeder Blanket of the control rods in the zone Z1 A and Z1 MAS.

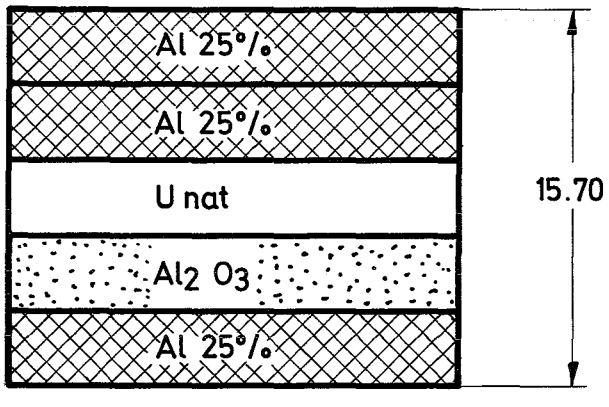

Fig. 1g Cells for the axial Breeder Blanket

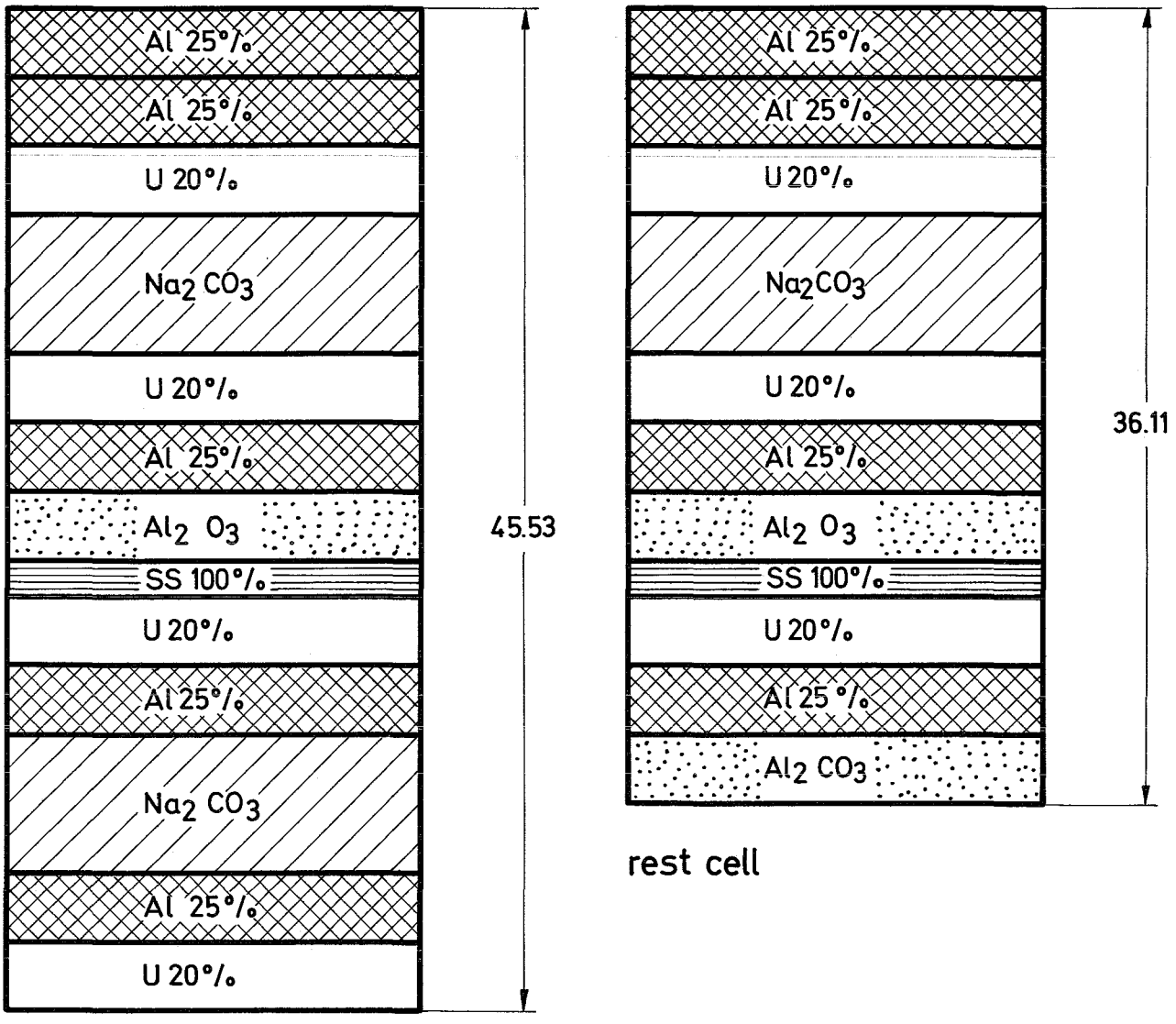

normal cell

rest cell

Fig. 2 Unit Cell for SNEAK Control Rods

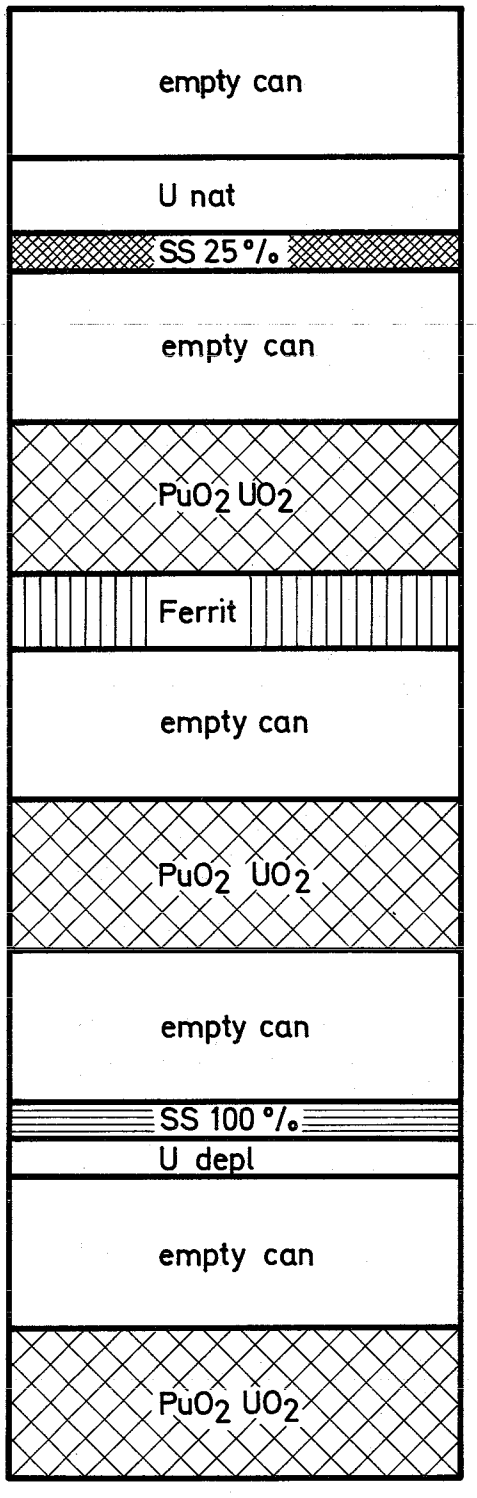

Fig.3 Voided Cell of the Zone Z1 A

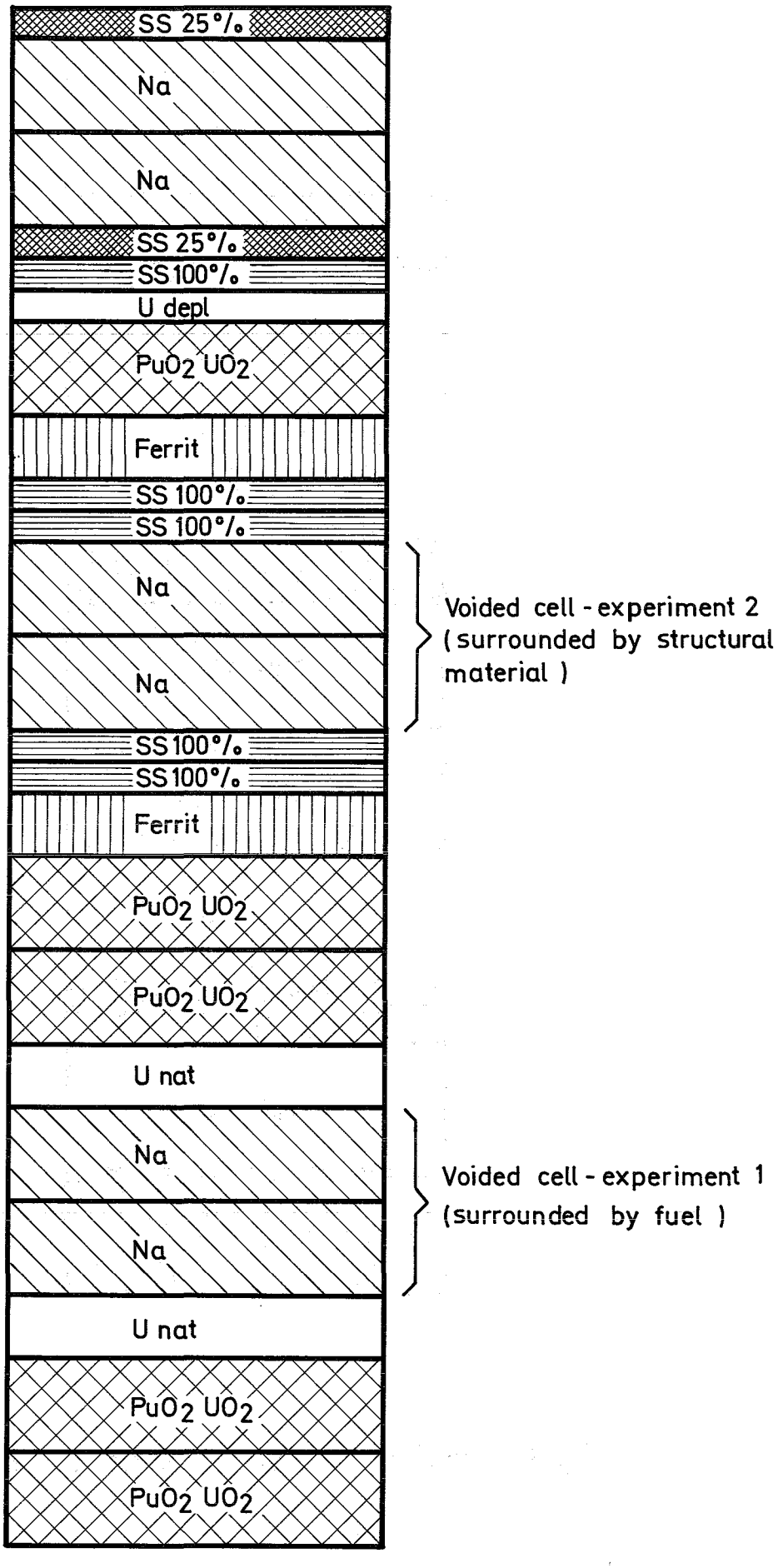

Fig. 4 Cell in the Pile - Oscillator - Element for Na-Void-Experiment

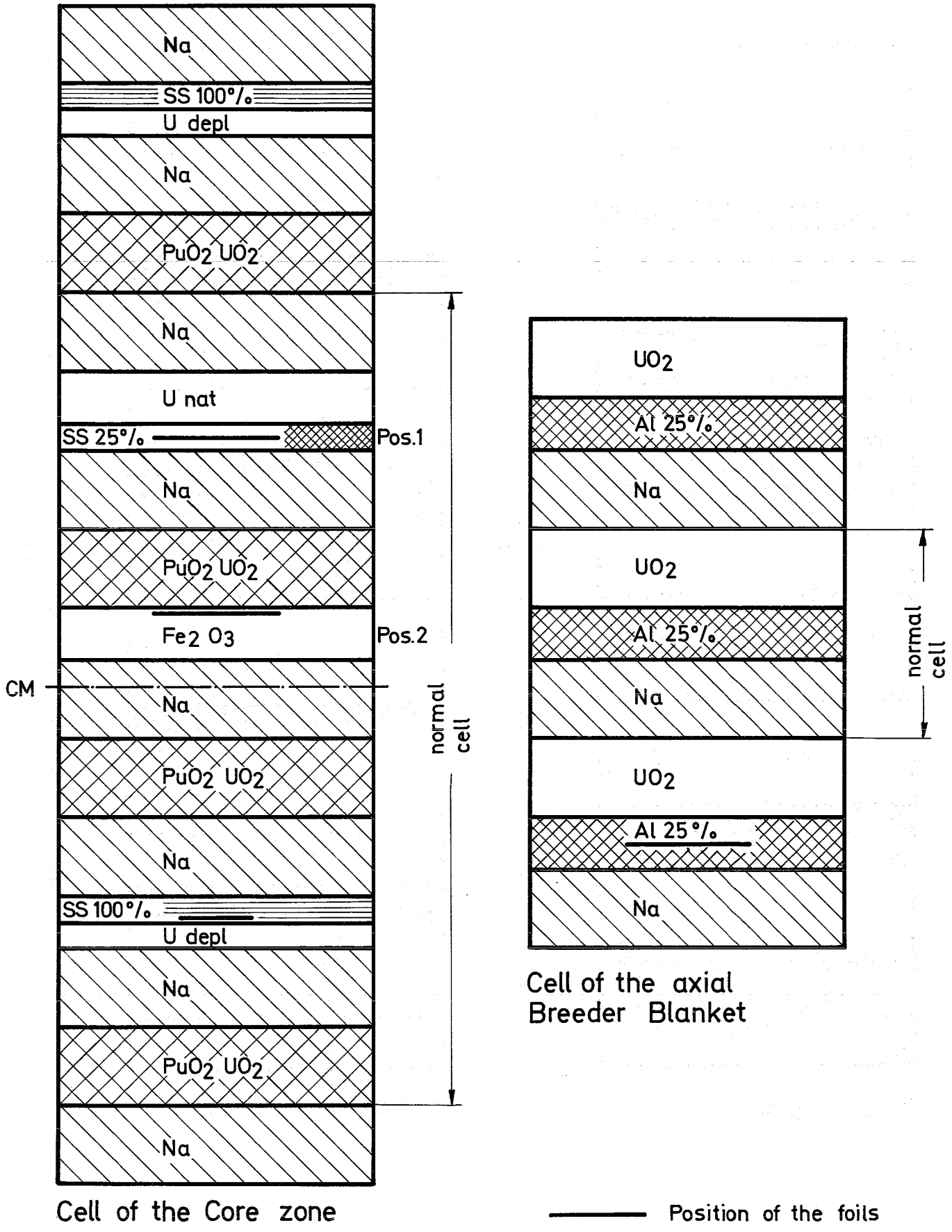

Fig.5 Position of the Foils in the Cells for the Reaction Rate - and fine Structure Measurements

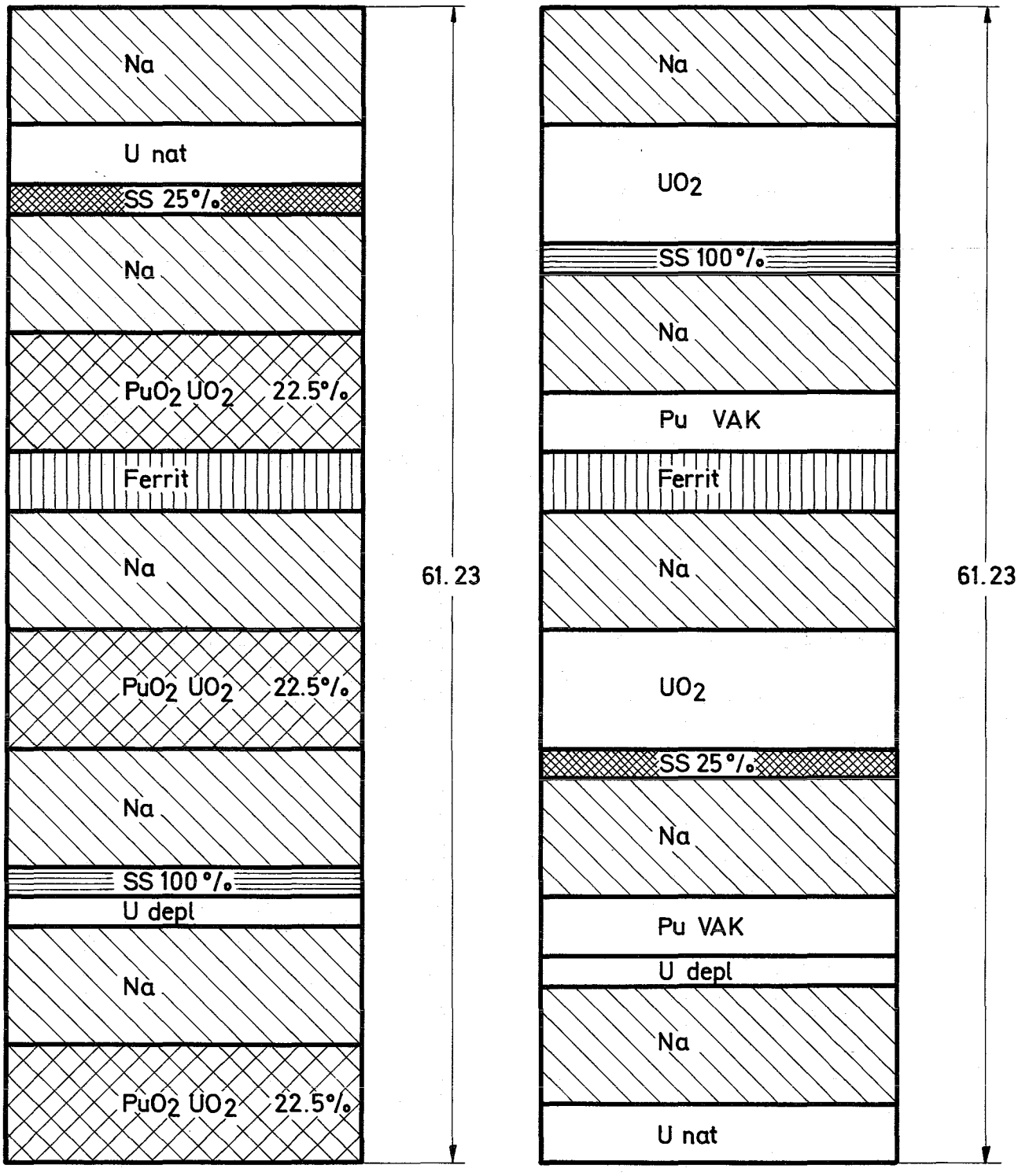

Pu 240 - zone

Pu 240 - buffer zone

Fig. 6 Unit Cells of the Pu 240- and Pu 240 - Buffer Zone

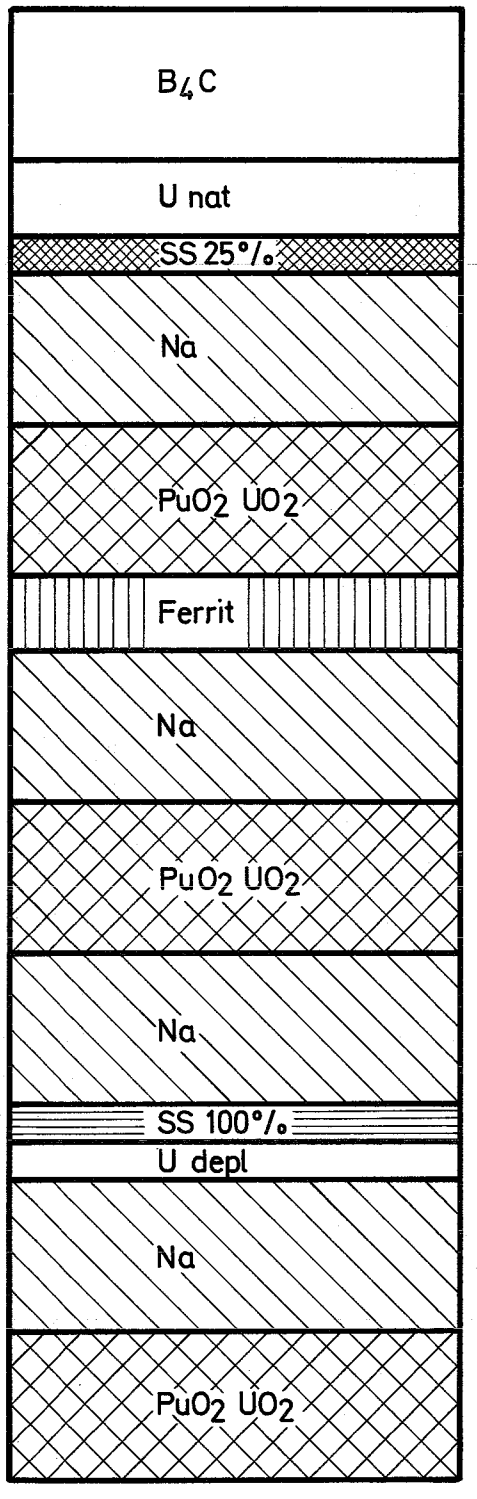

Fig.7 Unit Cell of the B_4C Zone

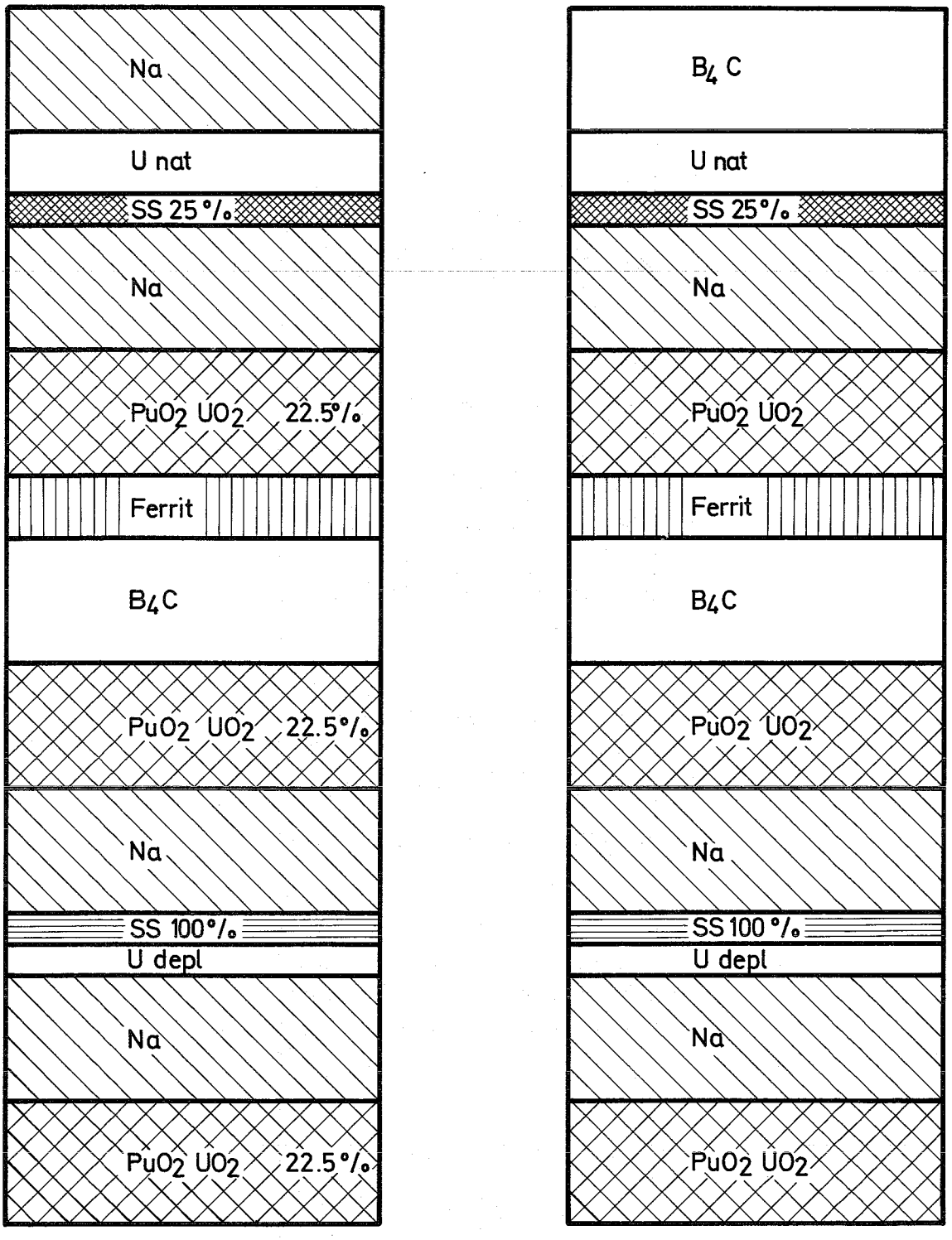

Pu 240 zone

B_4C zone

Fig. 8 Cells for the Measurement of the Reactivity Worth of Boron

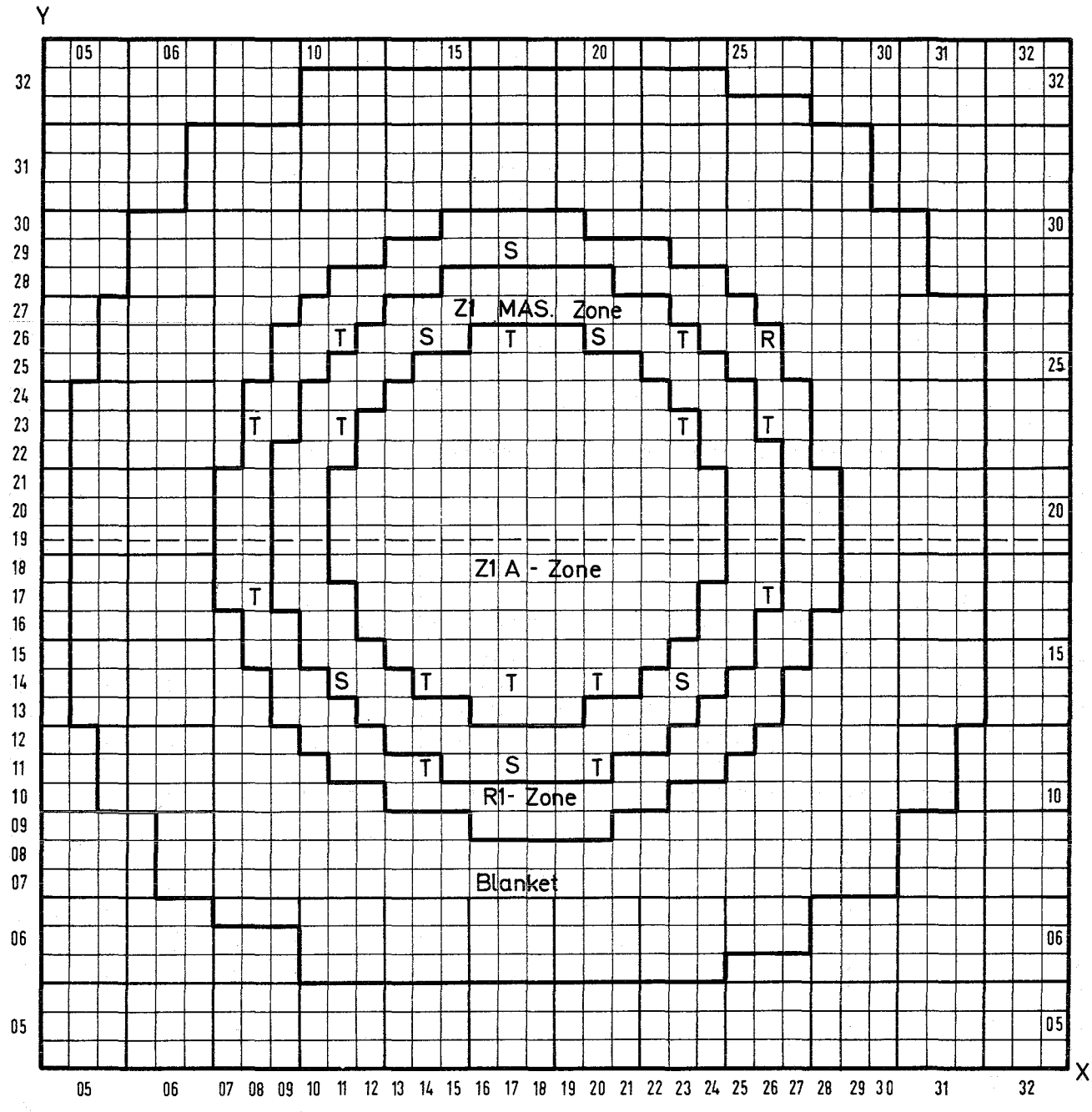

SNEAK-6A Cross Section of the Critical Configuration

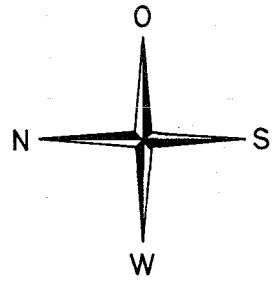

S = Safety rod
T = Shim rod
R = Control rod

———— Radial channel

Fig. 9

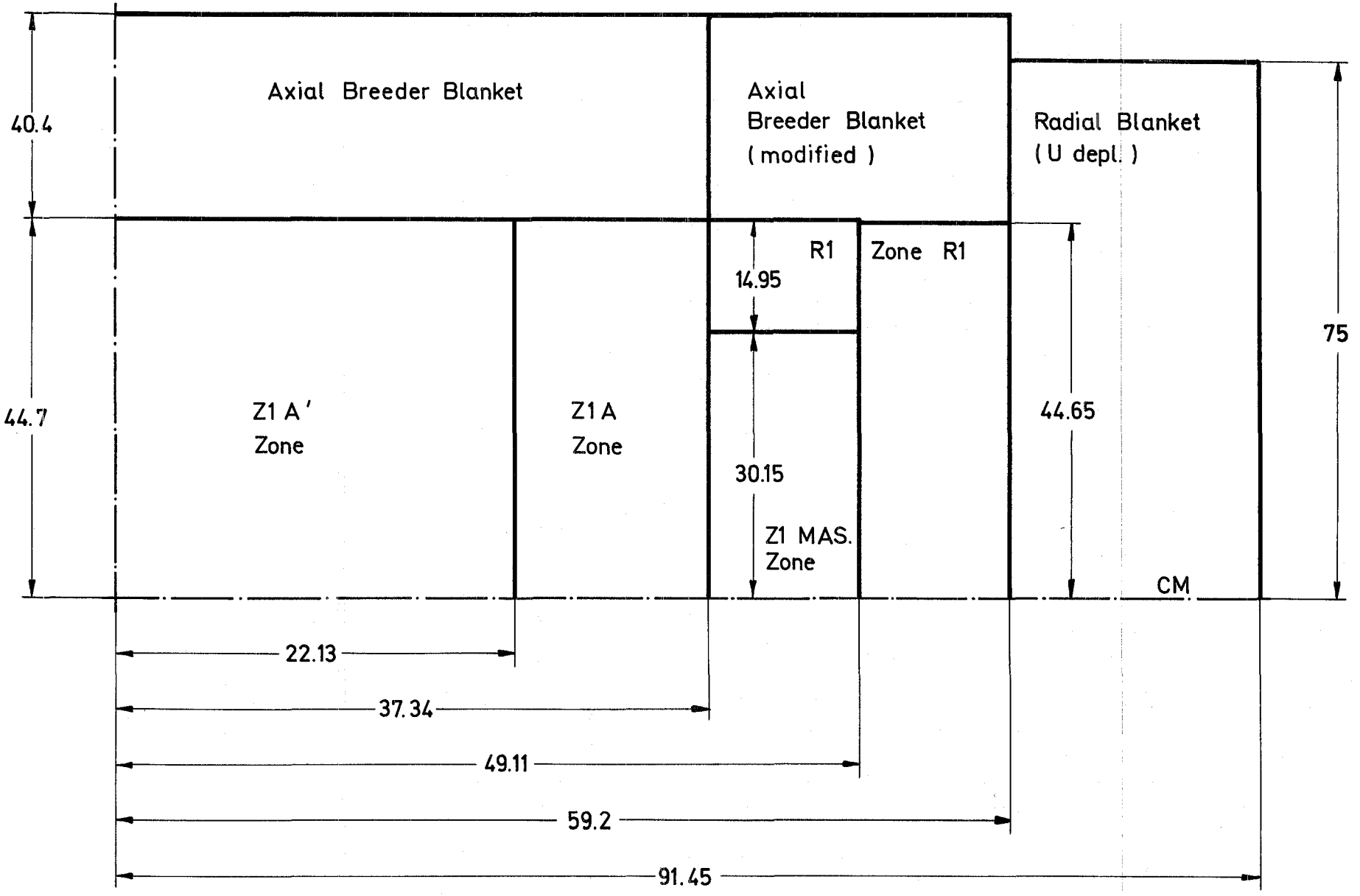

Fig. 10 Axial Cut through a Quarter of the Critical Core SNEAK-6A

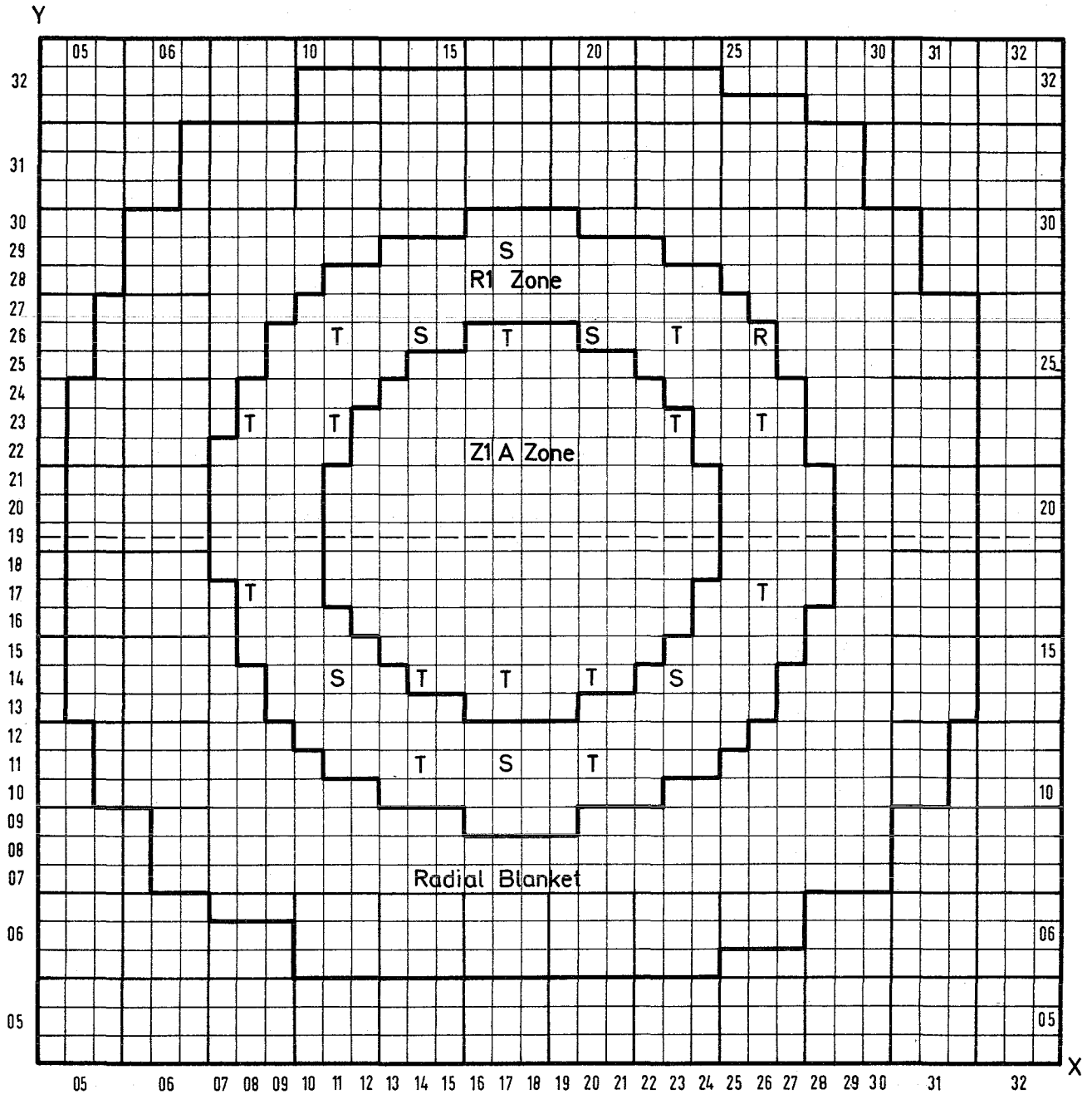

SNEAK - 6B

Cross Section of the Critical Configuration

S = Safety rod

T = Shim rod

R = Fine control rod

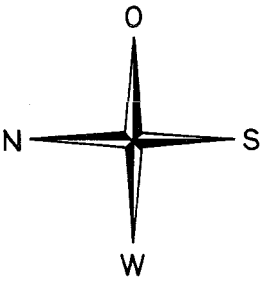

Fig. 11

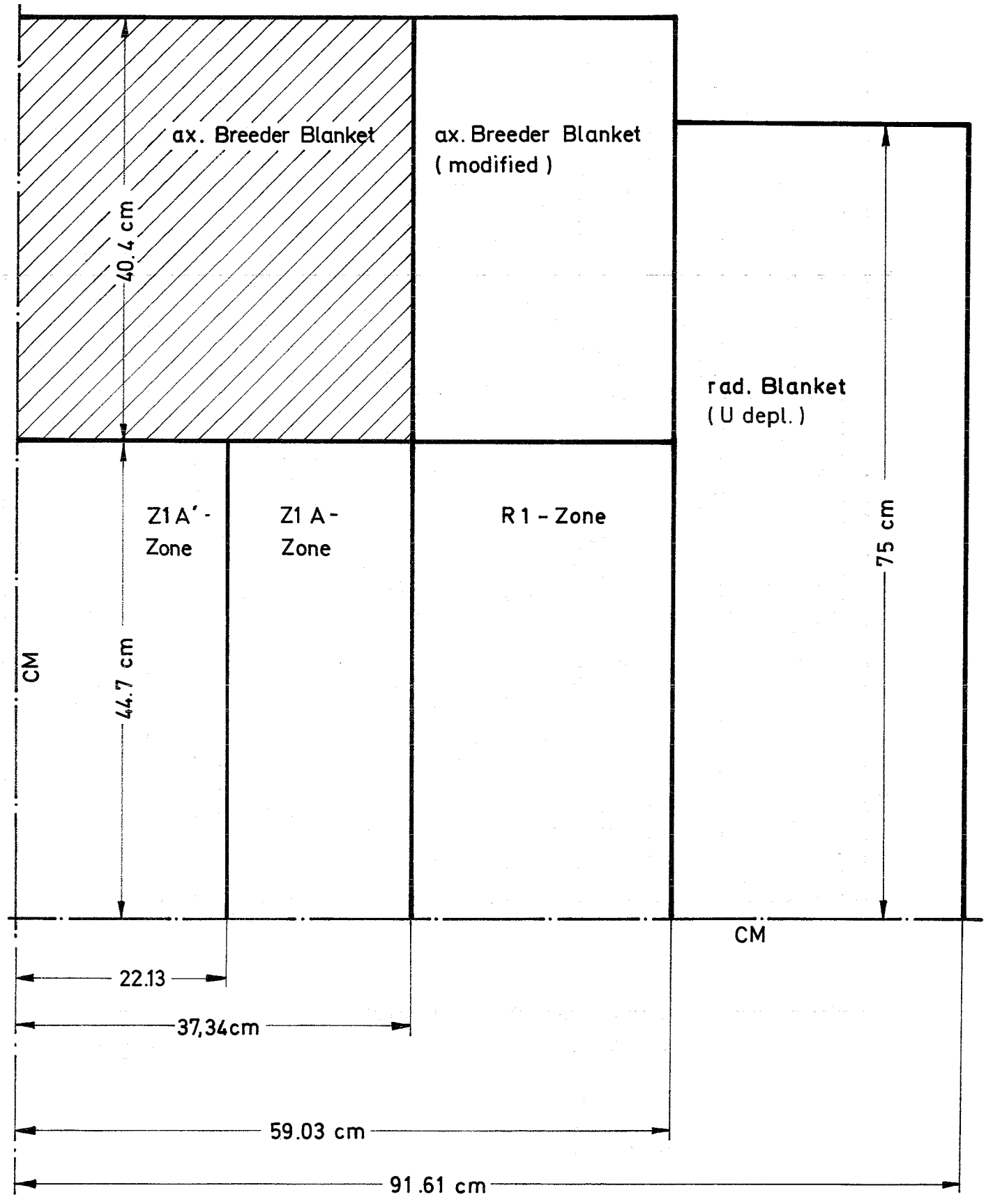

Fig.12 Axial Cut through a Quarter of the Critical Core SNEAK-6B

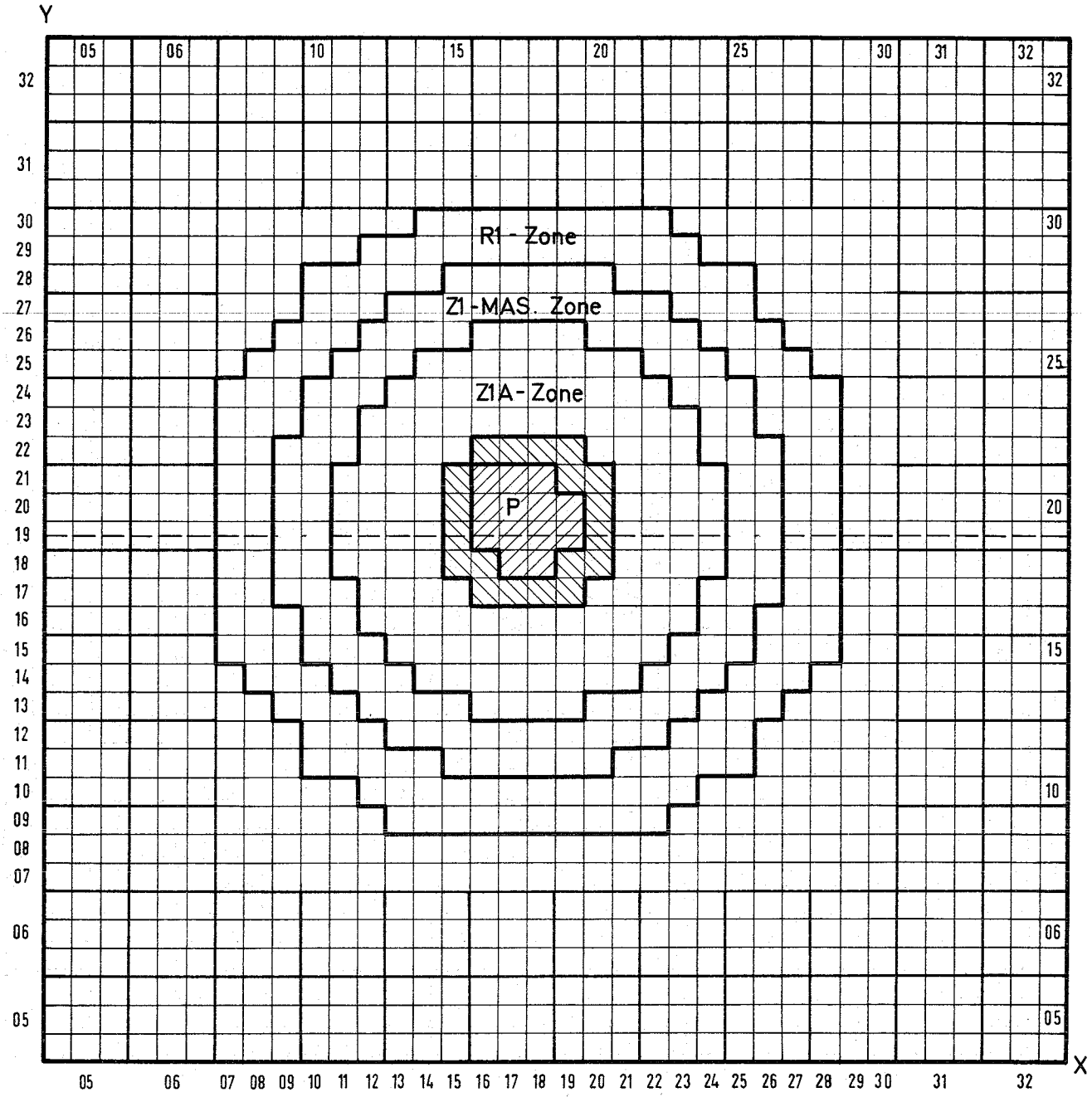

SNEAK - 6A Position of the Pu 240 Zone

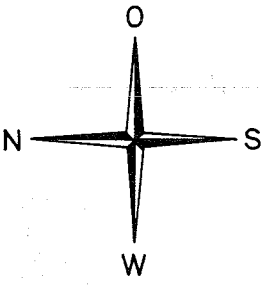

P Pile oscillator

Pu 240 zone

Buffer zone (VAK - Pu)

Fig. 13

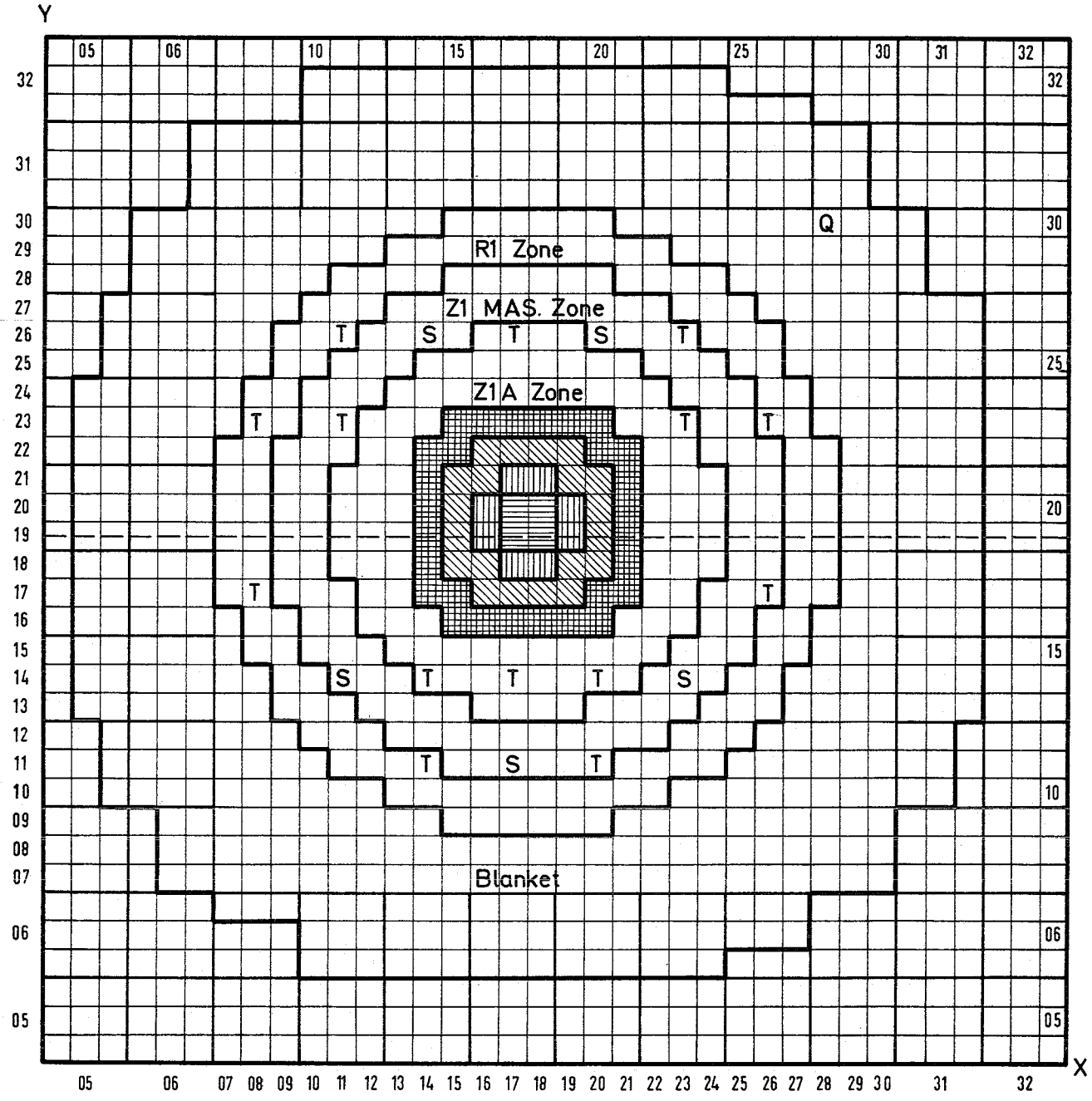

SNEAK - 6A Radial Na - Void Regions

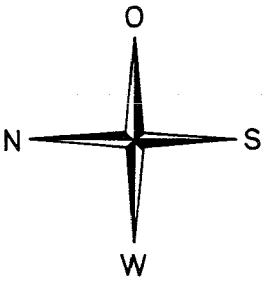

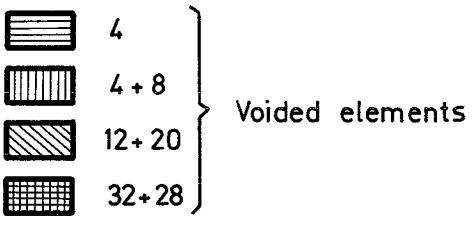

Fig. 14

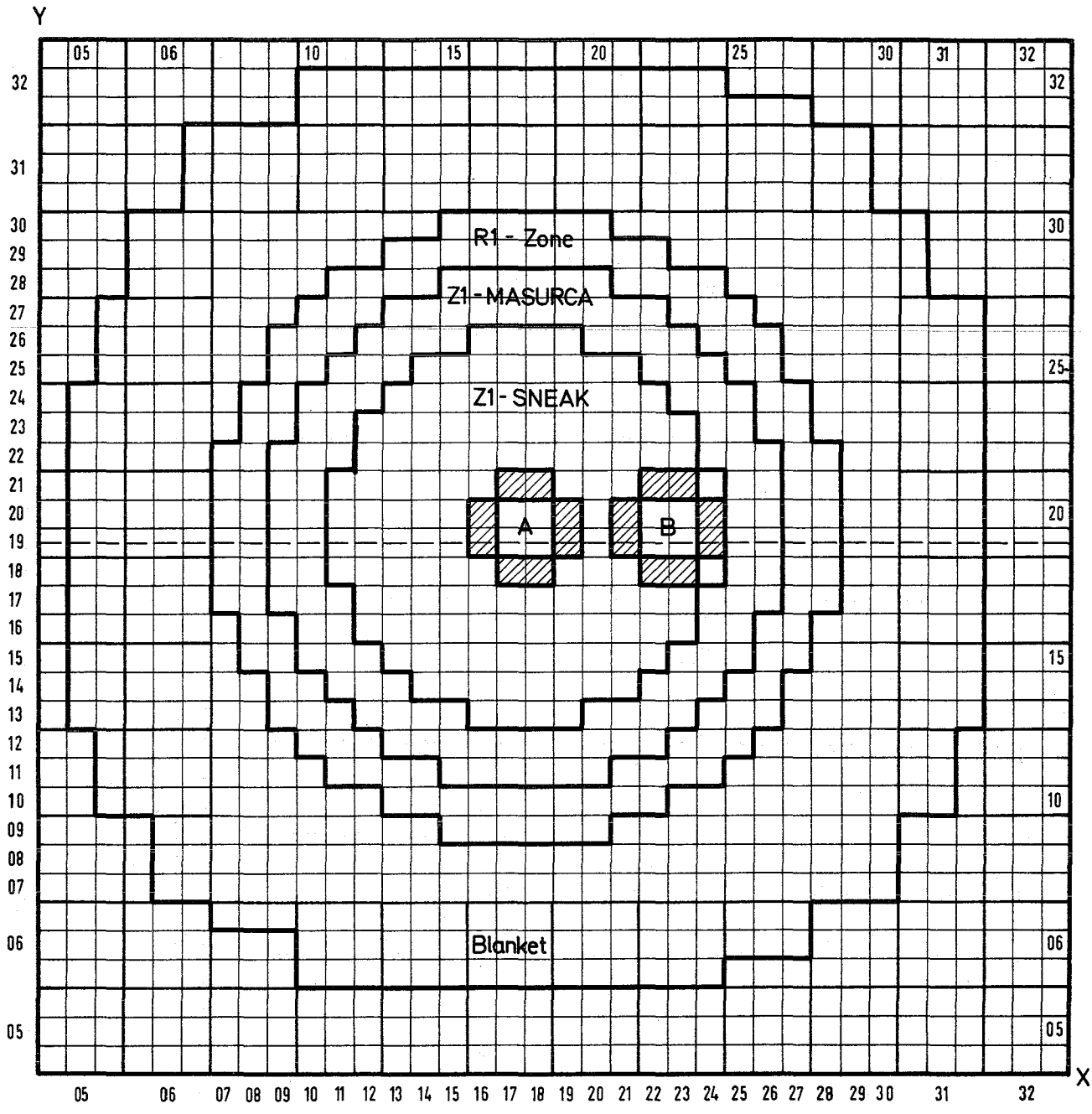

SNEAK - 6A CAVITIES

A) Central position
B) Off - center position

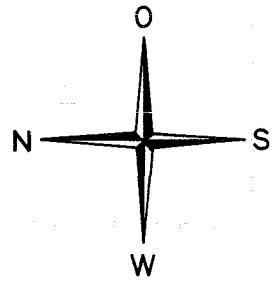

Fig. 15

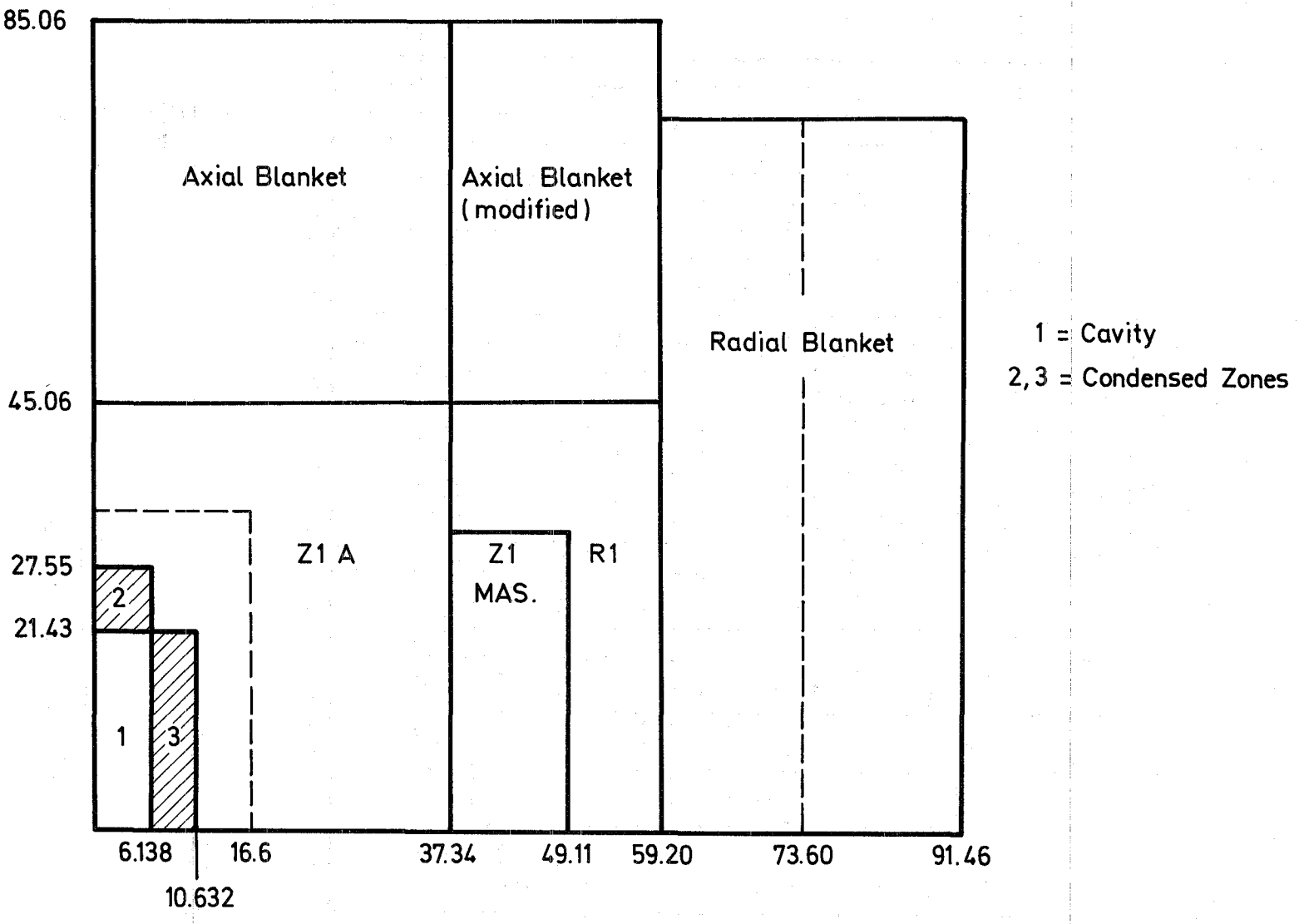

Fig. 16 SNEAK-6A Geometry for a central Cavity

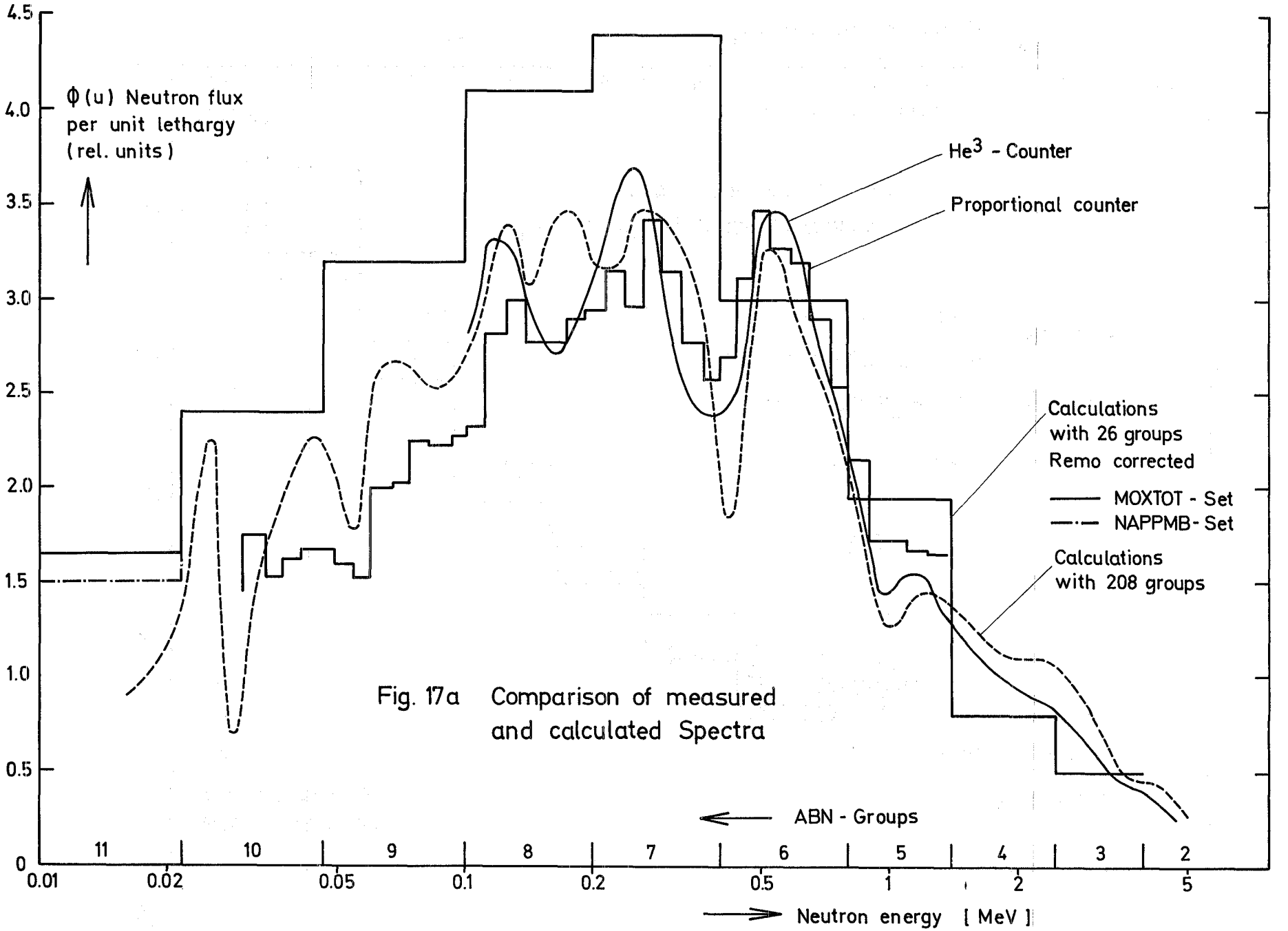

Fig. 17a Comparison of measured and calculated Spectra

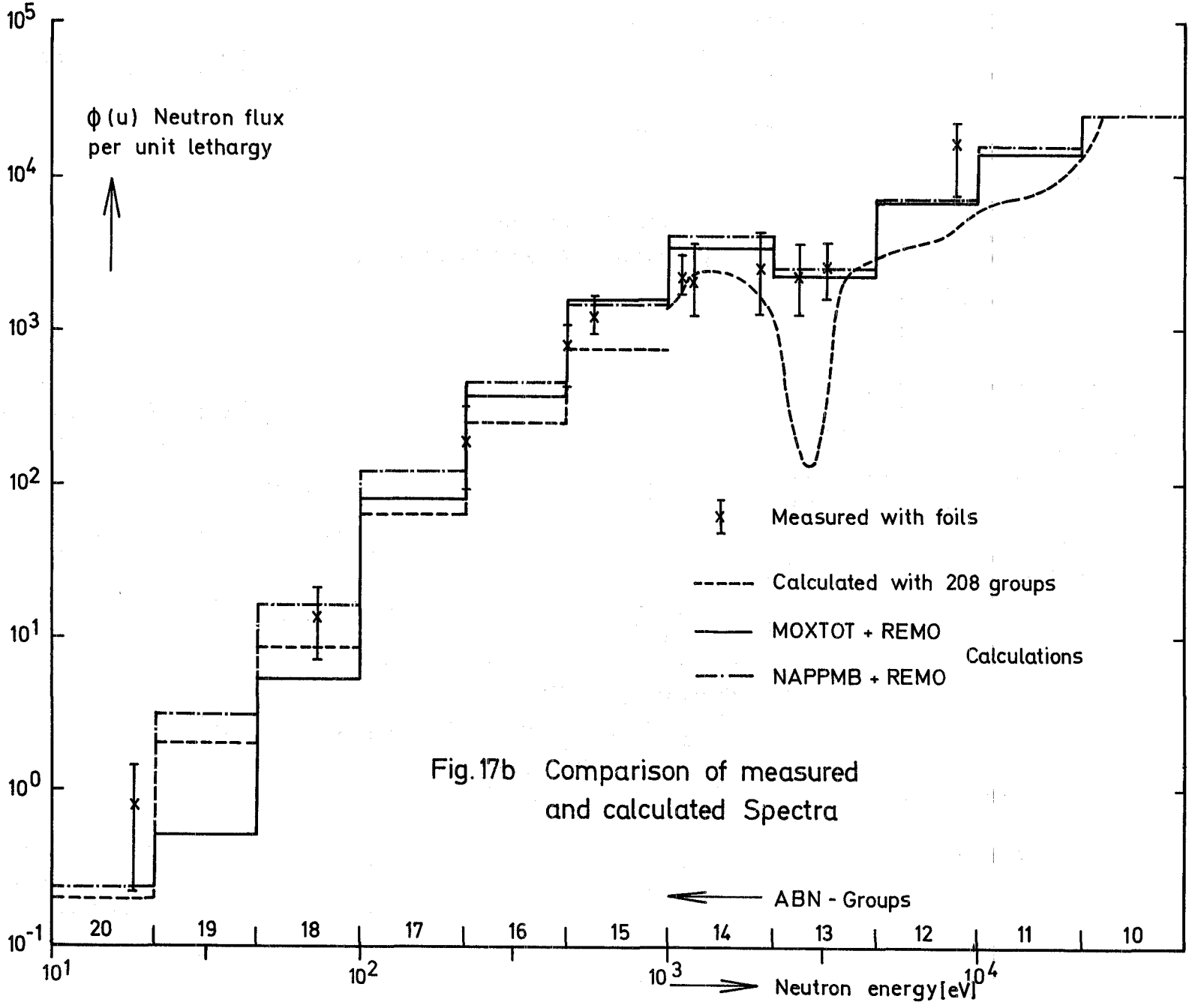

Fig. 17b Comparison of measured and calculated Spectra

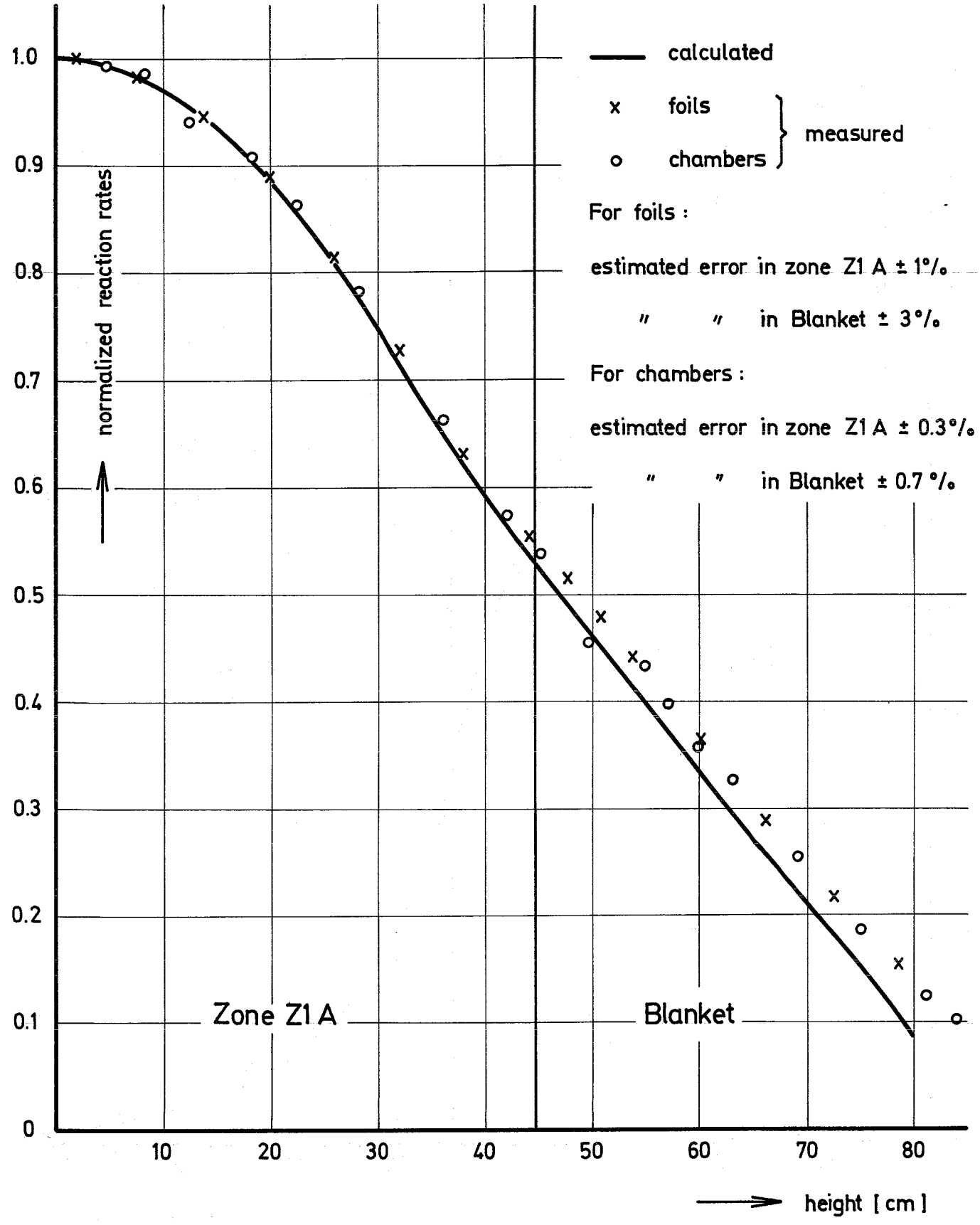

Fig. 18 SNEAK - 6A / 6B

Axial Fission Rate Traverse for U235

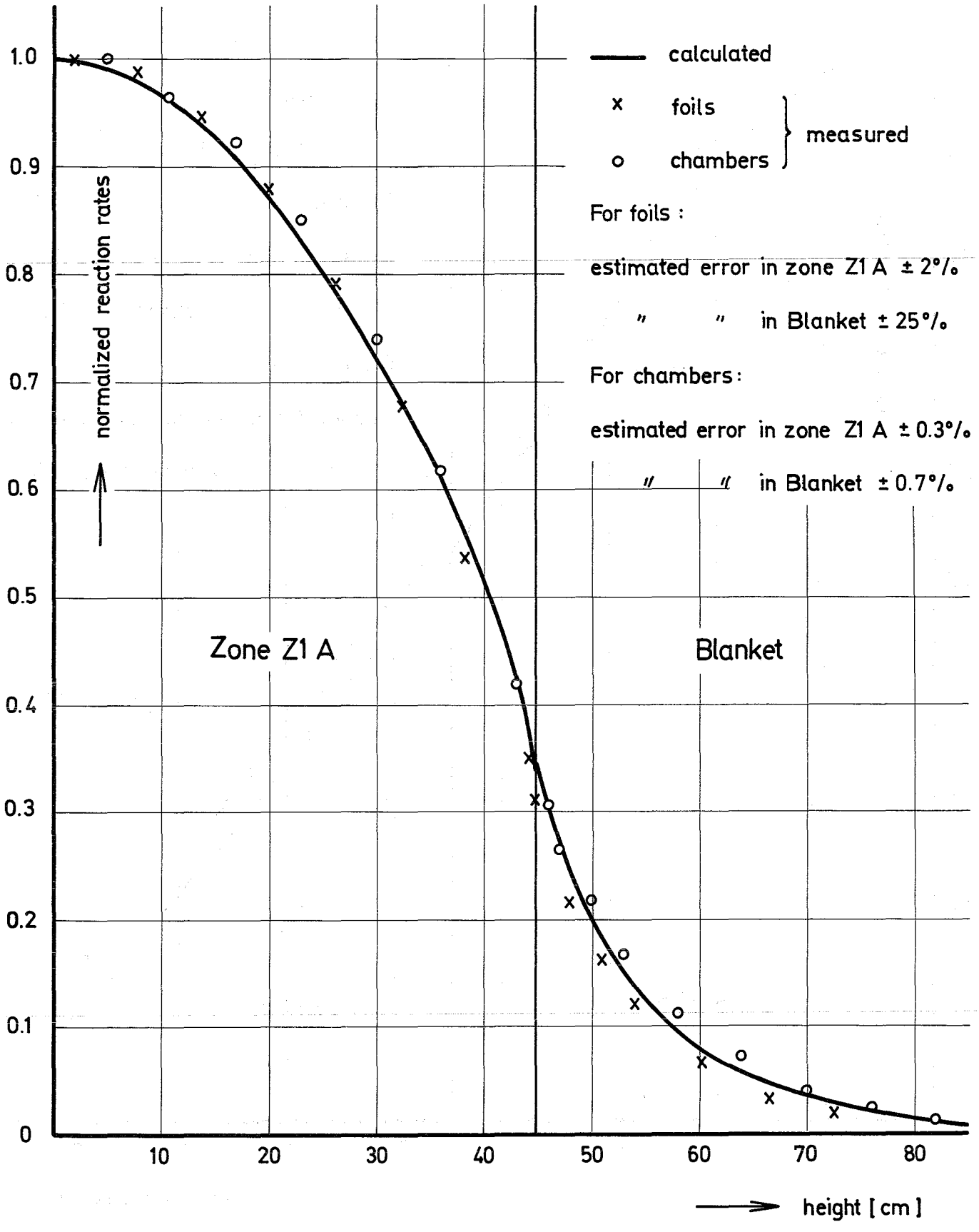

Fig. 19 SNEAK - 6A/6B

Axial Fission Rate Traverse for U 238

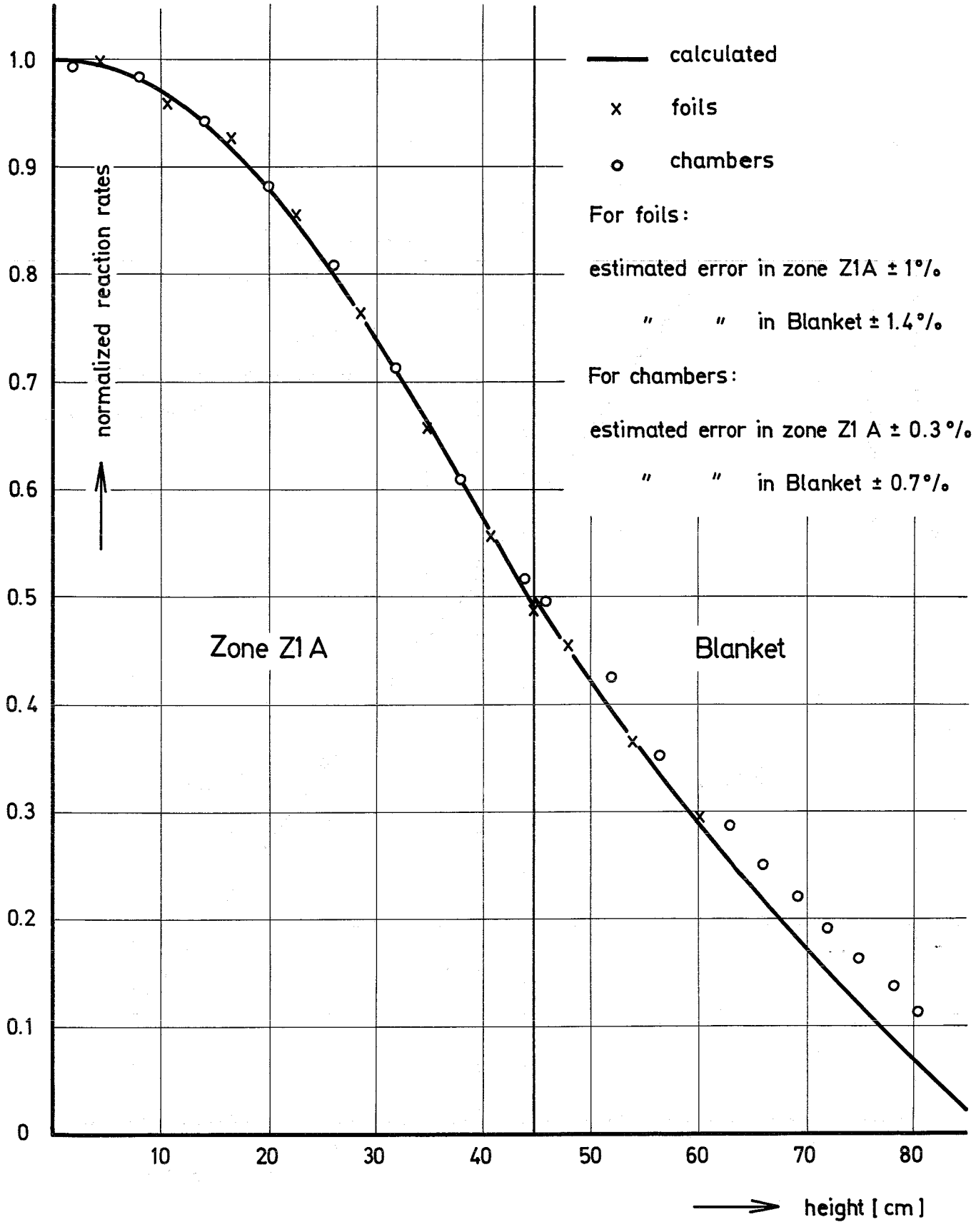

Fig. 20 SNEAK - 6A / 6B

Axial Fission Rate Traverse for Pu 239

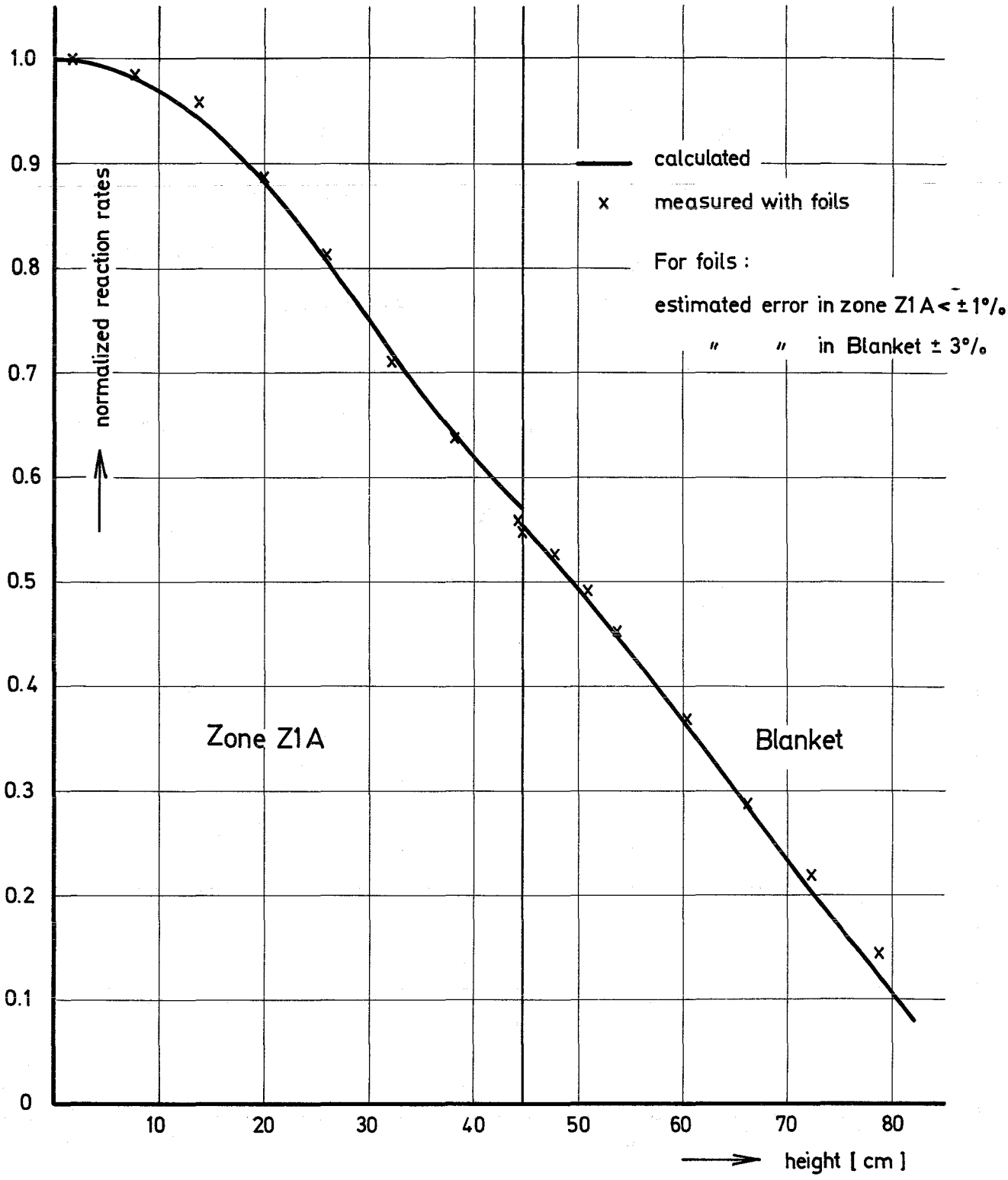

Fig. 21 SNEAK - 6A / 6B

Axial Capture Rate Traverse for U238

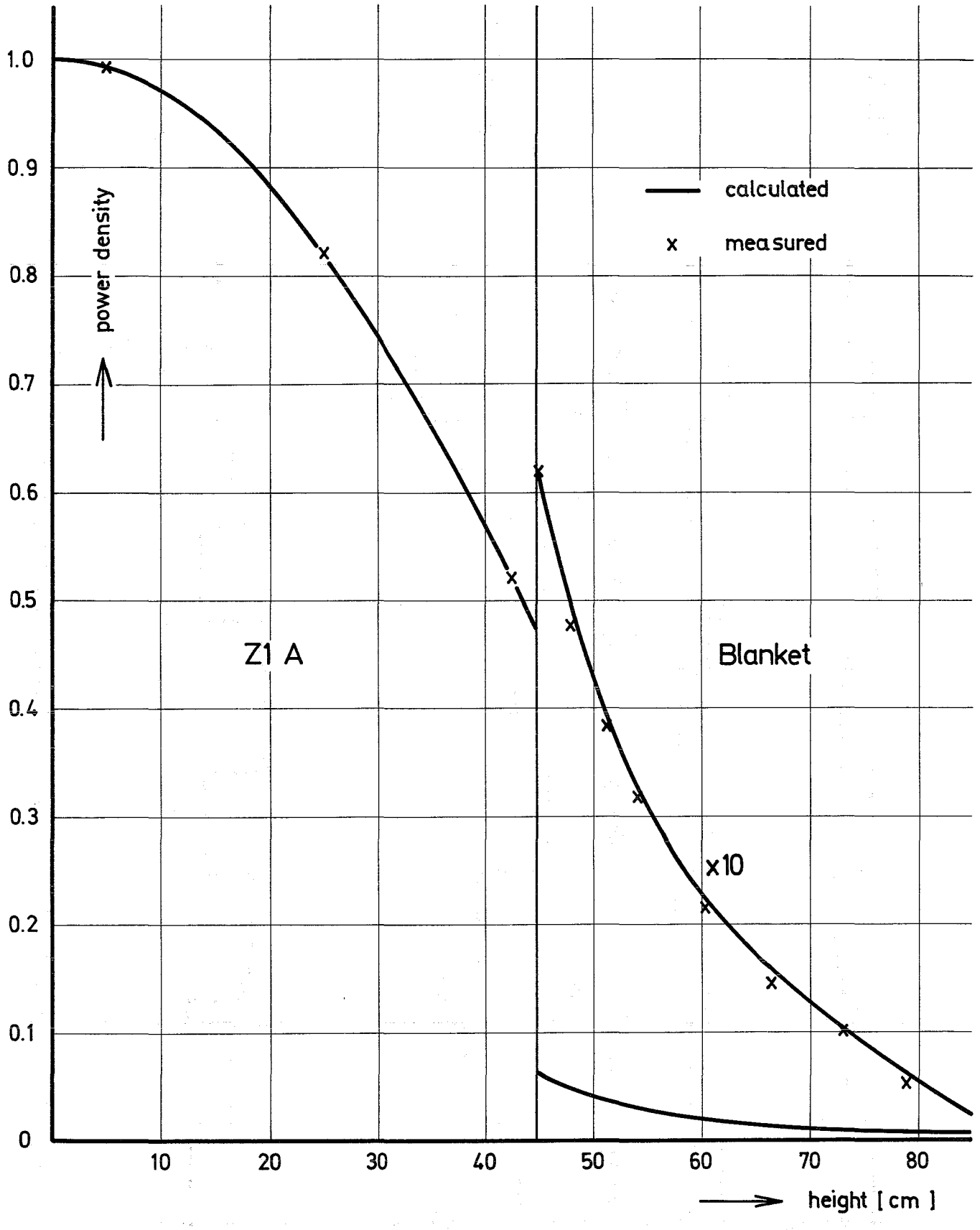

Fig.22 SNEAK - 6A / 6B

Axial Power Distribution

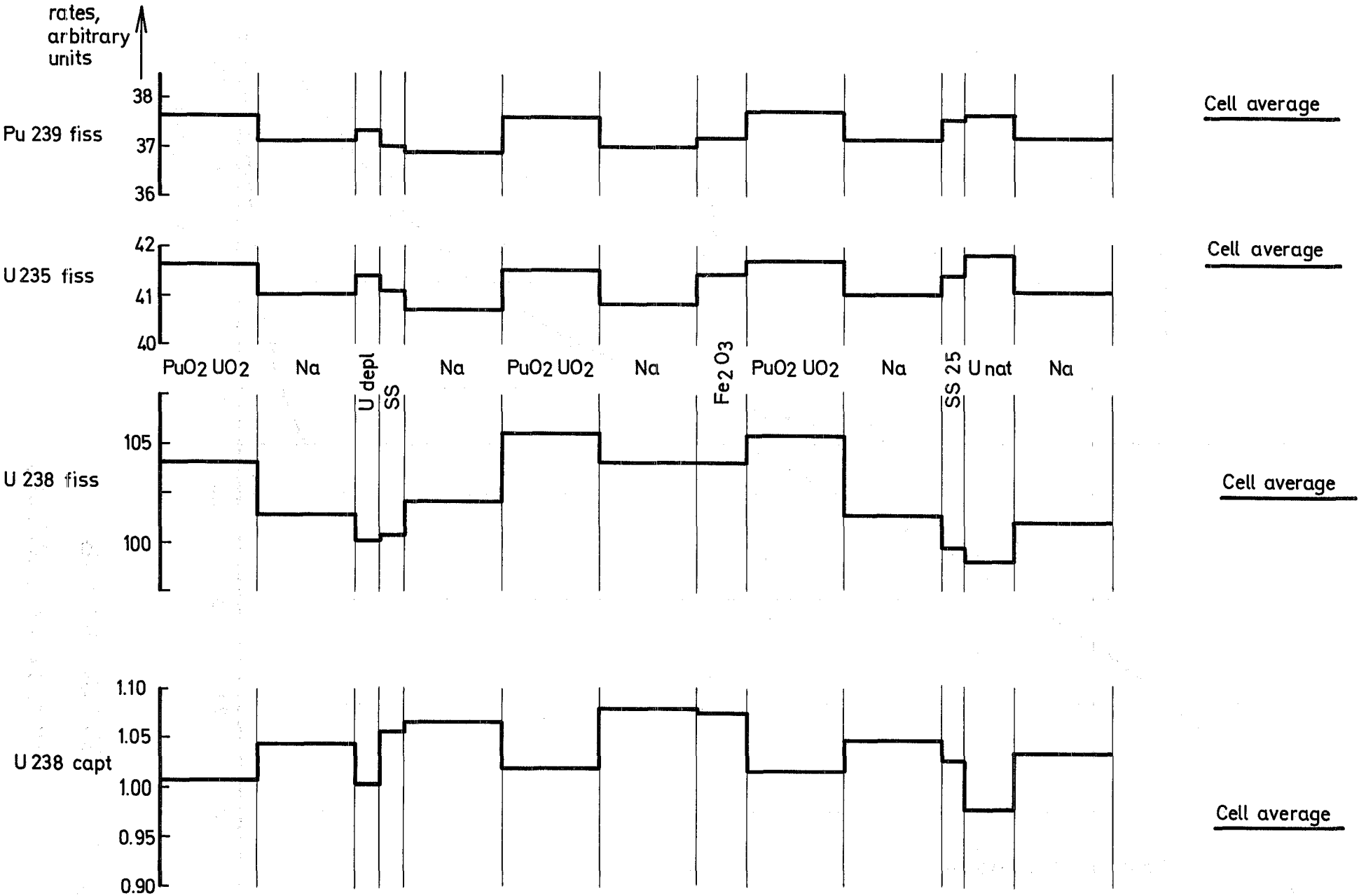

Fig. 23 SNEAK - 6A Cell fine Structure (calculated)

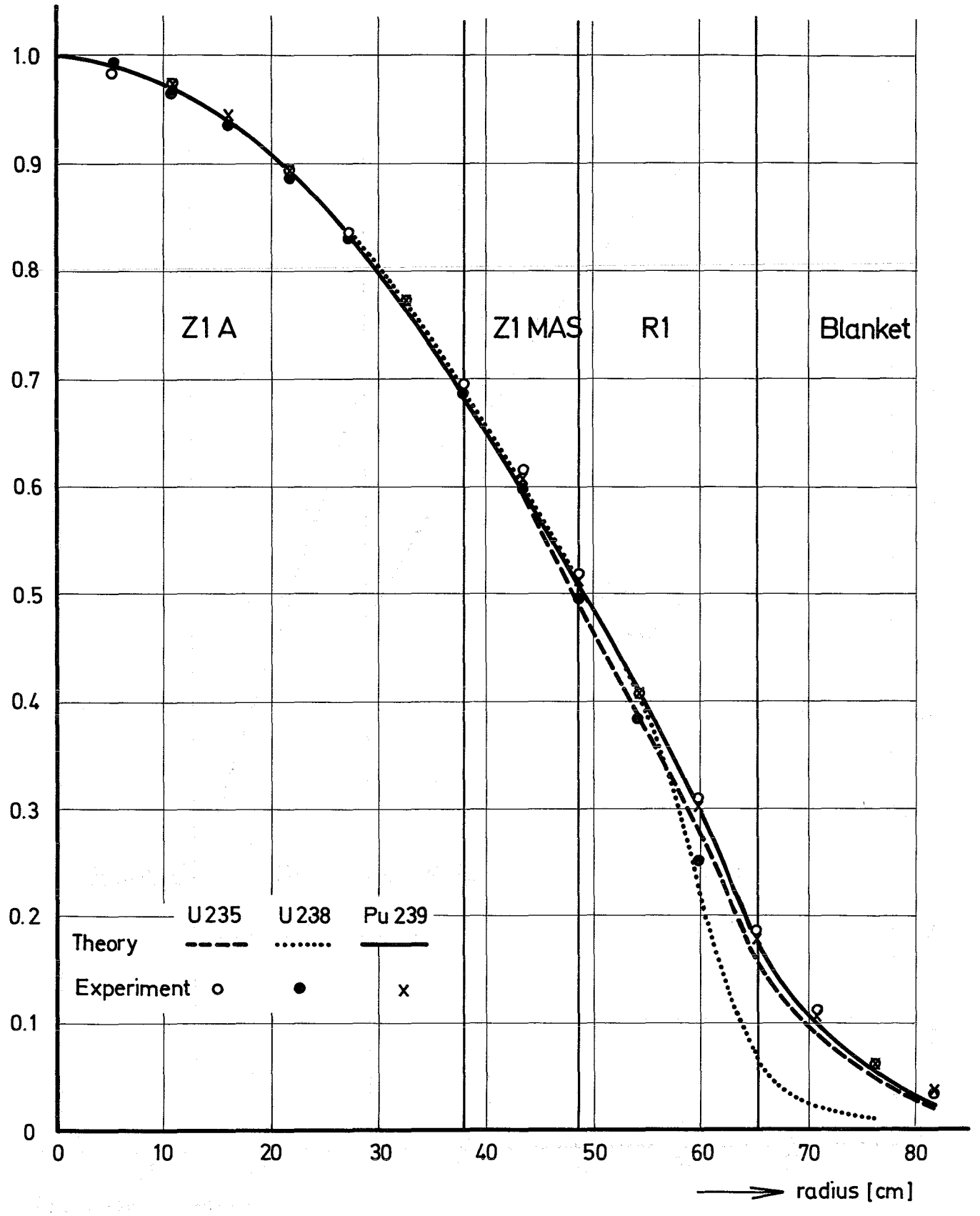

Fig. 24 Radial Fission Rate Traverses through SNEAK-6A

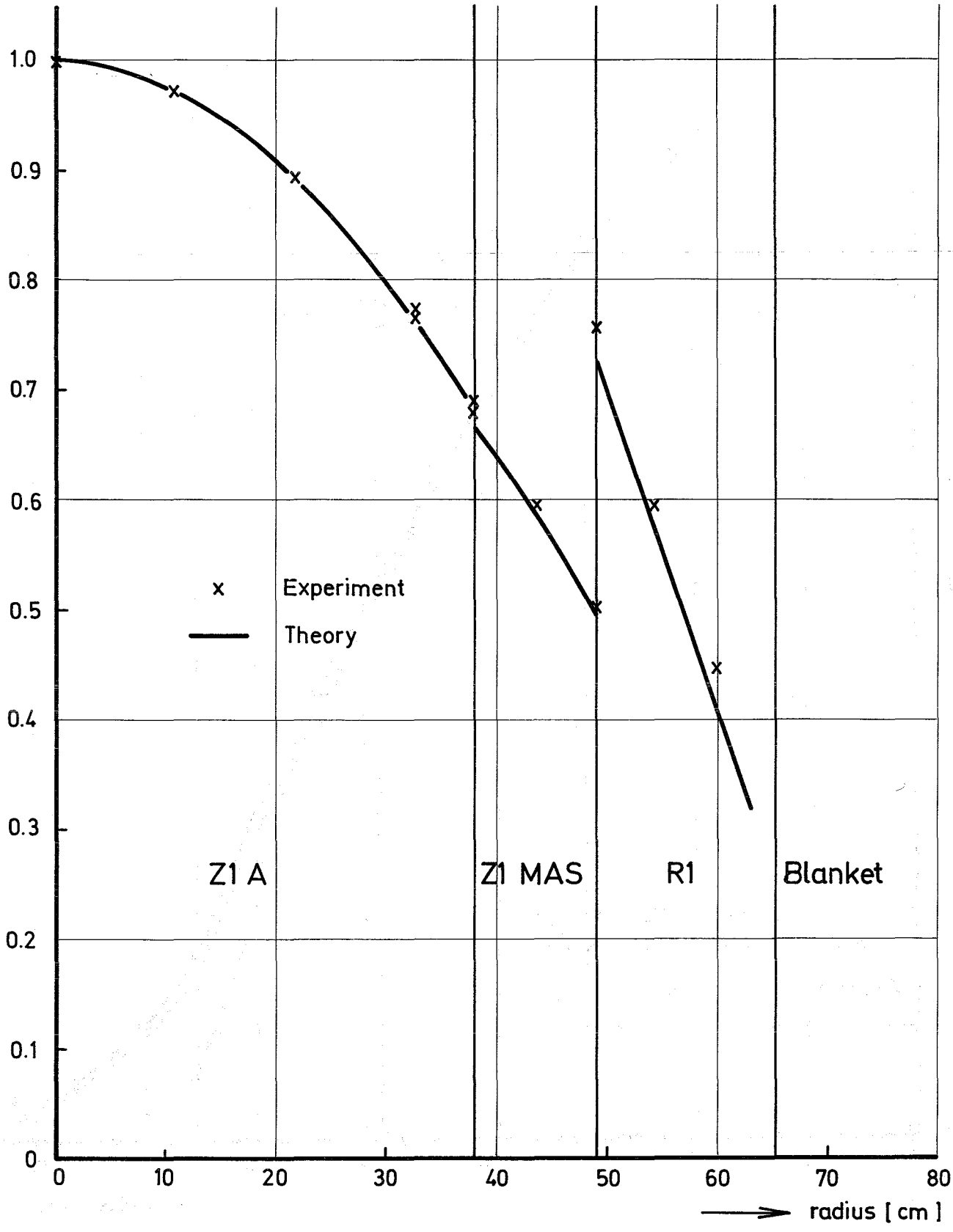

Fig. 25 Radial Power Density Traverse through SNEAK-6A

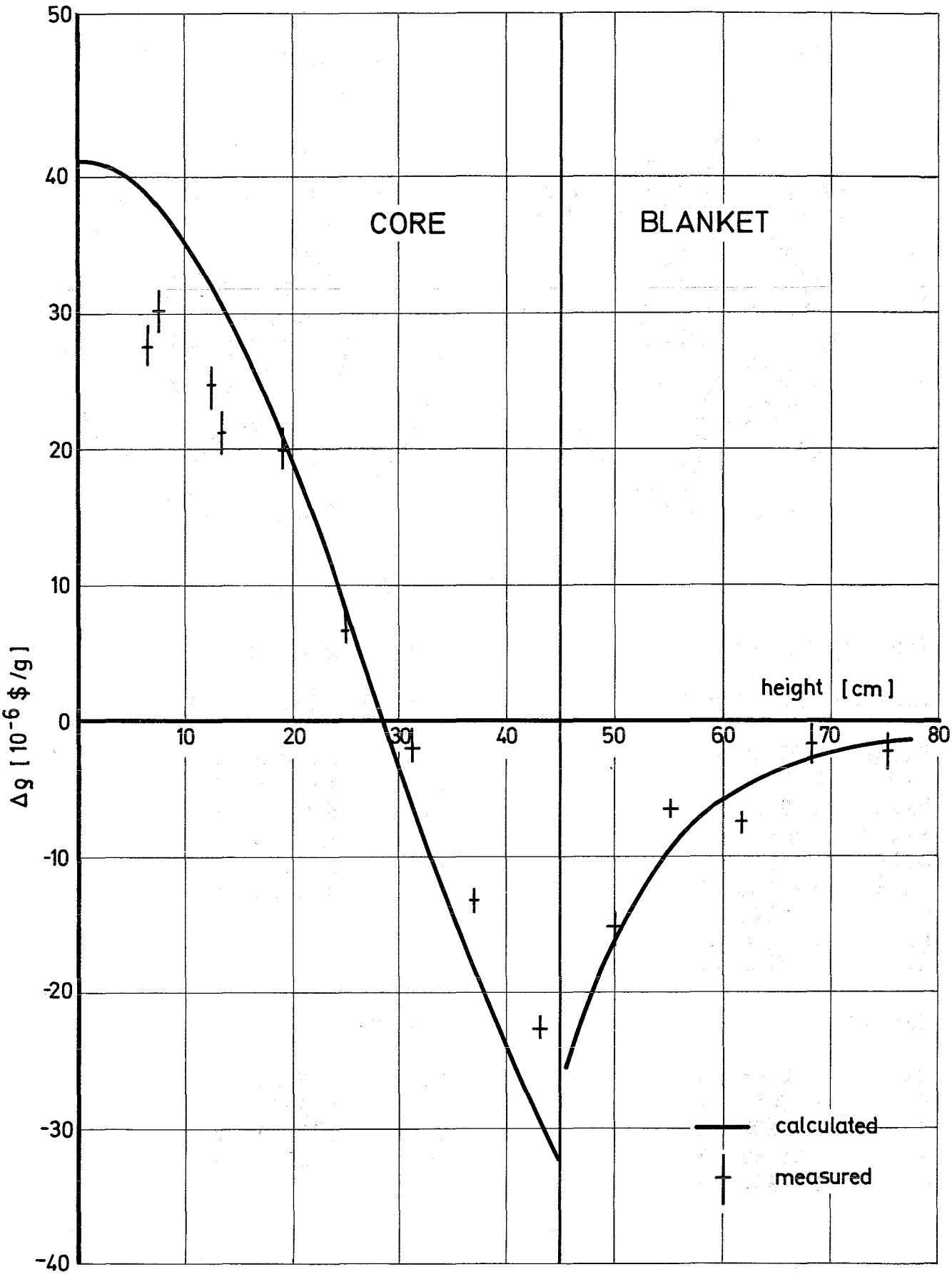

Fig. 26 Axial Na - Void Traverse

a) for Zone Z1M

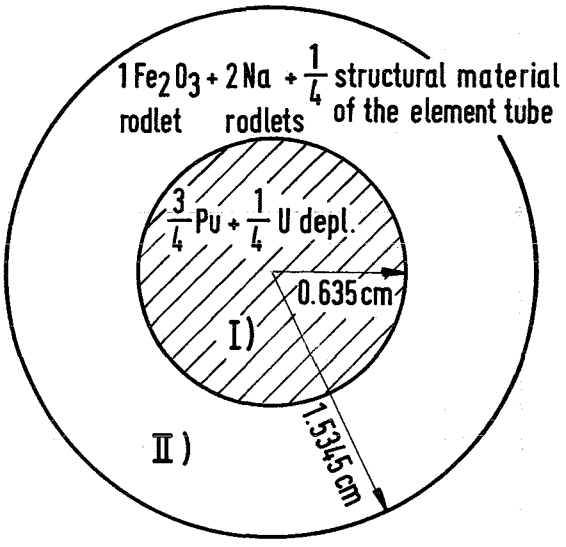

b) for the axial Breeder-Blanket

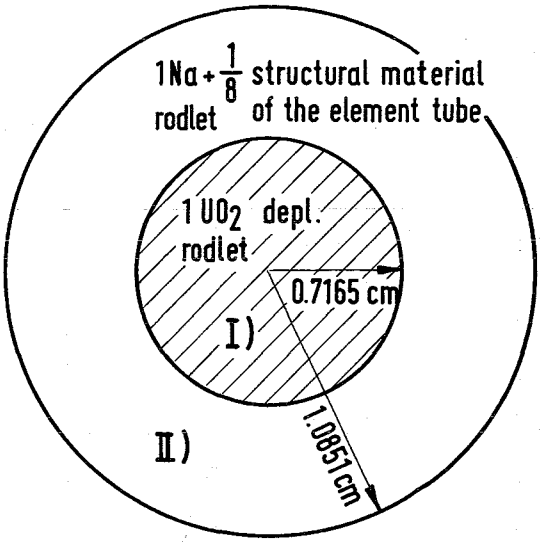

Atom densities for

Zone I): [10^{-24} cm^3]

Pu 239	7.06844 - 3
Pu 240	6.51900 - 4
Pu 241	6.18272 - 5
Pu 242	7.69638 - 6
U 235	9.36373 - 5
U 238	3.46269 - 2
Fe	4.16942 - 3
Cr	7.61260 - 4
Ni	8.82860 - 4

Zone II):

Na	1.06868 - 2
Fe	1.42812 - 2
Cr	3.99608 - 3
Ni	1.94659 - 3
O	1.39954 - 2

Atom densities for

Zone I): [10^{-24} cm^3]

U 235	8.37000 - 5
U 238	1.94724 - 2
Fe	6.23350 - 3
Cr	1.67400 - 3
Ni	8.23360 - 4
O	3.91120 - 2

Zone II):

Na	1.57054 - 2
Fe	1.08804 - 2
Cr	3.15870 - 3
Ni	1.52554 - 3

Fig. 27 Models for calculating the Heterogeneity

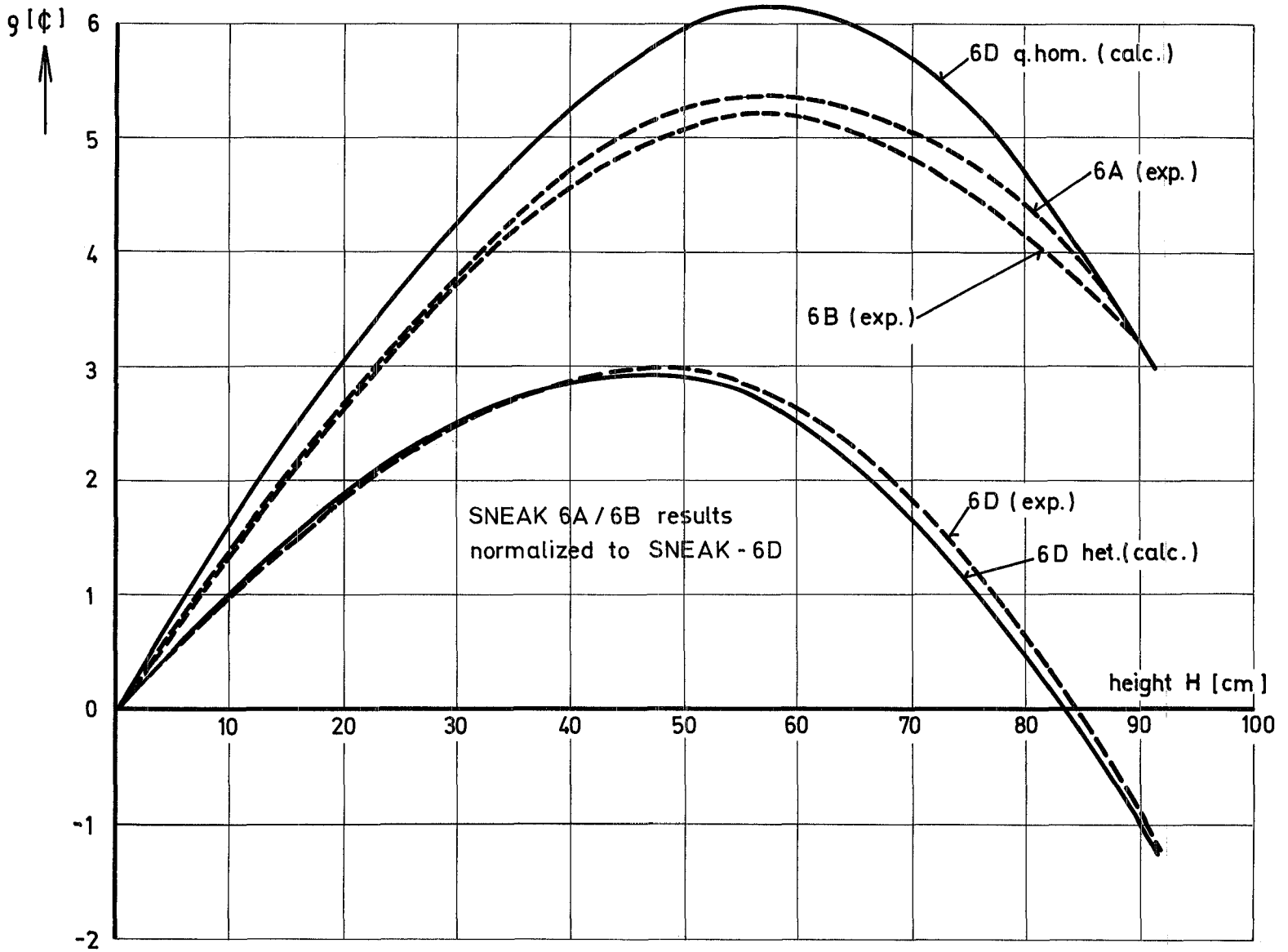

Fig.28 Experimental Reactivity Change, ϱ, as a Result of Voiding four Central Elements of SNEAK - 6A / 6B / 6D up to a Height H and Corresponding Calculations for SNEAK - 6D